TUNNEL LOCATION BY MAGNETOMETER, ACTIVE SEISMIC, AND RADON DECAY METHODS

ALEXANDRIA LABORATORIES REPORT NO.: AL-75-1

W. C. Dean

18 June 1975

Teledyne Geotech
314 Montgomery Street
Alexandria, Virginia 22314

REPORT DOCUMENTATION PAGE		READ INSTRUCTIONS BEFORE COMPLETING FORM
1. REPORT NUMBER AL-75-1	2. GOVT ACCESSION NO.	3. RECIPIENT'S CATALOG NUMBER
4. TITLE (and Subtitle) TUNNEL LOCATION BY MAGNETOMETER, ACTIVE SEISMIC, AND RADON DECAY METHODS		5. TYPE OF REPORT & PERIOD COVERED Technical 6. PERFORMING ORG. REPORT NUMBER
7. AUTHOR(s) W. C. Dean		8. CONTRACT OR GRANT NUMBER(s) F08606-74-C-0013
9. PERFORMING ORGANIZATION NAME AND ADDRESS Teledyne Geotech 314 Montgomery Street Alexandria, Virginia 22314		10. PROGRAM ELEMENT, PROJECT, TASK AREA & WORK UNIT NUMBERS
11. CONTROLLING OFFICE NAME AND ADDRESS Defense Advanced Research Projects Agency Nuclear Monitoring Research Office 1400 Wilson Blvd.- Arlington, Virginia 22209		12. REPORT DATE 18 June 1975 13. NUMBER OF PAGES 84
14. MONITORING AGENCY NAME & ADDRESS(if different from Controlling Office) VELA Seismological Center 312 Montgomery Street Alexandria, Virginia 22314		15. SECURITY CLASS. (of this report) Unclassified 15a. DECLASSIFICATION DOWNGRADING SCHEDULE

16. DISTRIBUTION STATEMENT (of this Report)

APPROVED FOR PUBLIC RELEASE; DISTRIBUTION UNLIMITED.

17. DISTRIBUTION STATEMENT (of the abstract entered in Block 20, if different from Report)

18. SUPPLEMENTARY NOTES

19. KEY WORDS (Continue on reverse side if necessary and identify by block number)

Tunnel location
Proton Magnetometer
Seismic location
Radon detection

20. ABSTRACT (Continue on reverse side if necessary and identify by block number)

This project investigated three methods of detecting mines or tunnels in granite: magnetic, seismic, and radioactive decay of radon.

The magnetic, using a proton precession magnetometer, aims to detect tunnels from the magnetic materials (rails, roof bolts, wiring) these mines are expected to contain. This method works for both surface and borehole surveys when the sensor is less than 20 feet from the magnetic source. For deeper rails a surface survey will probably not be successful since the rail

anomalies are not of one sign but oscillate above and below the mean background level with wavelengths on the order of two rail lengths. Such anomalies cannot be distinguished from weak geologic anomalies.

The active seismic methods aims to detect tunnels by reflection or refraction of P-waves from the tunnel or by reverberations of the tunnel walls. These experiments were unsuccessful due to insufficient high frequency energy being coupled into the rock containing the tunnel. Some evidence of cavity wall reverberations appeared over a coal mine, but the tunnel was shallow (15 feet) and the medium (coal) had a lower seismic velocity than granite.

The radon decay method aims to detect tunnelling activity by the extra release of radon gas freed into the atmosphere. For a tunnelling rate of 16 cubic meters per day, this method will fail due to a poor signal-to-noise ratio relative to all of the other sources of radon in the atmosphere.

ABSTRACT

This project investigated three methods of detecting mines or tunnels in granite: magnetic, seismic, and radioactive decay of radon.

The magnetic, using a proton precession m[illegible]tometer, aims to detect tunnels from the magnetic materials (rails, r[illegible]lts, wiring) these mines are expected to contain. This method works [illegible]ch surface and borehole surveys when the sensor is less than 20 feet from the magnetic source. For deeper rails a surface survey will probably not be successful since the rail anomalies are not of one sign but oscillate above and below the mean background level with wavelengths on the order of two rail lengths. Such anomalies cannot be distinguished from weak geologic anomalies.

The active seismic methods aims to detect tunnels by reflection or refraction of P-waves from the tunnel or by reverberations of the tunnel walls. These experiments were unsuccessful due to insufficient high frequency energy being coupled into the rock containing the tunnel. Some evidence of cavity wall reverberations appeared over a coal mine, but the tunnel was shallow (15 feet) and the medium (coal) had a lower seismic velocity than granite.

The radon decay method aims to detect tunnelling activity by the extra release of radon gas freed into the atmosphere. For a tunnelling rate of 16 cubic meters per day, this method will fail due to a poor signal-to-noise ratio relative to all of the other sources of radon in the atmosphere.

TABLE OF CONTENTS

LIST OF FIGURES

LIST OF FIGURES (Continued)

LIST OF FIGURES (Continued)

EXECUTIVE SUMMARY

This project investigated three geophysical methods of detecting underground mines or tunnels. The three methods are magnetic, seismic, and radioactive decay (of radon).

The magnetic method aims to detect mines from the magnetic anomalies generated by the rails these mines are all expected to contain. Other magnetic material in mines might include electrical wiring and structural material such as roof bolts and steel reinforcement bars in concrete slabs.

We conducted magnetic surveys with a proton precession magnetometer directly over railroad rails (sensor height eight feet), and over railroad tunnels where the rails were buried 50 to 100 feet below the magnetometer. In addition we drilled a borehole which passed within 12 feet of a mine and ran a magnetic survey with a borehole sensor.

The results show that the rails do exhibit strong magnetic anomalies (up to 1500 gamma for mainline railroad rails). However the magnetic anomalies are not constant as we had expected but oscillate above and below the background magnetic field of the earth with wavelengths comparable to the length of the rail sections. This oscillation further obscures what was already expected to be a small anomaly amongst the much larger geologic anomalies which are ever present. Moreover in the U.S.A. the railroad tunnels invariably are accompanied by fences and phone lines running over the tunnel parallel with the rails. These create surface anomalies, which are readily detected by the magnetometer, but further obscure the weak rail anomalies. Even without the confusion of parallel fences and phone lines, detection of rails in a mine by a surface magnetometer survey is doubtful even for mine (rail) depths of 15 to 50 feet.

In contrast the magnetometer shows strong anomalies, and oftentimes quite erratic behavior on repeated readings, when the sensor is close (a few inches to a few feet) to magnetic materials. The borehole survey showed just this behavior as the sensor passed the roof bolts and reinforcements in the experimental mine of the Colorado School of Mines. The erratic behavior

is especially pronounced when there are loops of magnetic material nearby (such as wire mesh or barbwire looped around a fencepost). The reason is that the pulsing of the magnetometer creates an electromagnet out of the magnetic wire loop where the residual effect varies from reading to reading.

Thus borehole magnetic surveys do show some promise of detecting mines from the magnetic material contained in them although, when successful, the strongest magnetic anomalies may not be coming from the rails.

The seismic method aims to detect tunnels by reflection or refraction of P-waves from the tunnel. For this method to work effectively, the seismic wavelengths in rock should be comparable or shorter than the cross-section dimensions of the target. Even for railroad tunnels (15 feet by 25 feet) the wavelengths of seismic energy used in geophysical exploration are much longer than the tunnel dimensions.

Our field experiments show very little high frequency energy (100 to 500 Hz) coupled into the rocks resulting in no reflection evidence of the tunnels. This was true when we used Dinoseis, or dynamite caps, or a sledge hammer (used with the Bison hammer seismograph). The problem at the sites over the two railroad tunnels in Colorado was due to a low velocity layer on the surface trapping almost all of the energy preventing any significant penetration into the granite containing the tunnel.

Watkins (1967) reported on reverberations from underground cavity walls with a resonant frequency close to that predicted by Biot (1952). We did not see such reverberations from the railroad tunnels again due to the lack of energy penetrating the granite. However we did see such reverberations over a mine in coal (15 feet deep) on a Bison seismic profile. Although the coal tunnel is smaller (2x2 meters) than railroad tunnels, it is also shallow (5 meters) and exists in a uniform half space (coal) with a seismic velocity much less than that of granite.

For any subsequent experiments the field practice should make use of a multiple geophone system rather than a single sensor and hammer source such as the Bison. The correlation between traces is better when several traces are looking at seismic returns from the same source rather than one source per trace as in the Bison hammer seismograph.

The radon method aims to detect on-going tunnelling activity by detecting the release of radon gas freed into the atmosphere. All granite and crystaline rocks contain some uranium. Radon (Rn^{222}) is a daughter product of U^{238} and will be released to the atmosphere as the crushed rock from the mine is excavated.

Our study shows that for the amount of tunnelling expected (4 meters per day with a cross section of 2 x 2 meters), it is highly unlikely this method could detect radon from the tunnelling activity as opposed to all other sources of radon in the atmosphere, even under the most optimistic assumptions. With more realistic assumptions there is no hope.

INTRODUCTION

The objective of this project is to detect underground mines or tunnels by geophysical methods. The mines are expected to be approximately 2 x 2 meters in cross section, located in crystaline rocks such as granite, gneisses, or shists in hilly terrain, and with depths of burial of a few feet to as much as 200 feet or more.

This project has limited its attention to only three methods: detection of magnetic materials in the mine, reflection or refraction evidence of a tunnel by seismic exploration techniques, and detection of radon released to the atmosphere by the excavation activity. Other methods or techniques are considered outside the scope of this study.

MAGNETIC METHODS

The tunnels of interest are all expected to have rails. In addition they probably have electric wiring which may or may not be in use. In some locations, perhaps where the mines are shallow or in unconsolidated material, they may have roof bolts or iron reinforcements in concrete walls or ceilings.

The strength of magnetic dipoles decrease as the inverse cube of the distance (r^{-3}). However, rails are good approximations to infinitely long magnetic sources and so would be expected to decrease as the inverse square of the distance (r^{-2}). Figure 1 from the Geometrics Applications Manual for Portable Magnetometers (Breiner, 1973) is a nomogram showing the expected magnetic field strength from various types of objects versus the distance from the magnetometer. Note that the field strength from most objects vary as the inverse cube of the distance but that from pipelines vary as the inverse square.

In Figure 1 Breiner used the cross sectional area, A, of a pipeline as:

$$A = \pi Dt$$

where D is the diameter of pipeline (6") and t is the thickness (1/4"). Such a pipeline has a volume of 0.1 cubic feet per yard or approximately 50 pounds per yard. By comparison mainline rails are frequently 135 pounds per yard and mine rails are approximately 30 pounds per yard.

If we can detect infinitely long magnetic anomalies of 10 gamma, then we might expect to detect a 6-inch pipeline or a pair of mine rails buried at a depth of 40 feet. Other expected characteristics of our mine rail anomalies are that their expected direction is known and that their route will be roughly horizontal so the anomaly strength, will decrease with the square of the ground elevation (proportional to h^{-2}).

The equipment we used were proton precession magnetometers manufactured by Geometrics. These instruments can measure the earth's magnetic field accurately to within one or two gammas. We used both a base station with a recorder (Model G-826) and a portable unit (Model G-816).

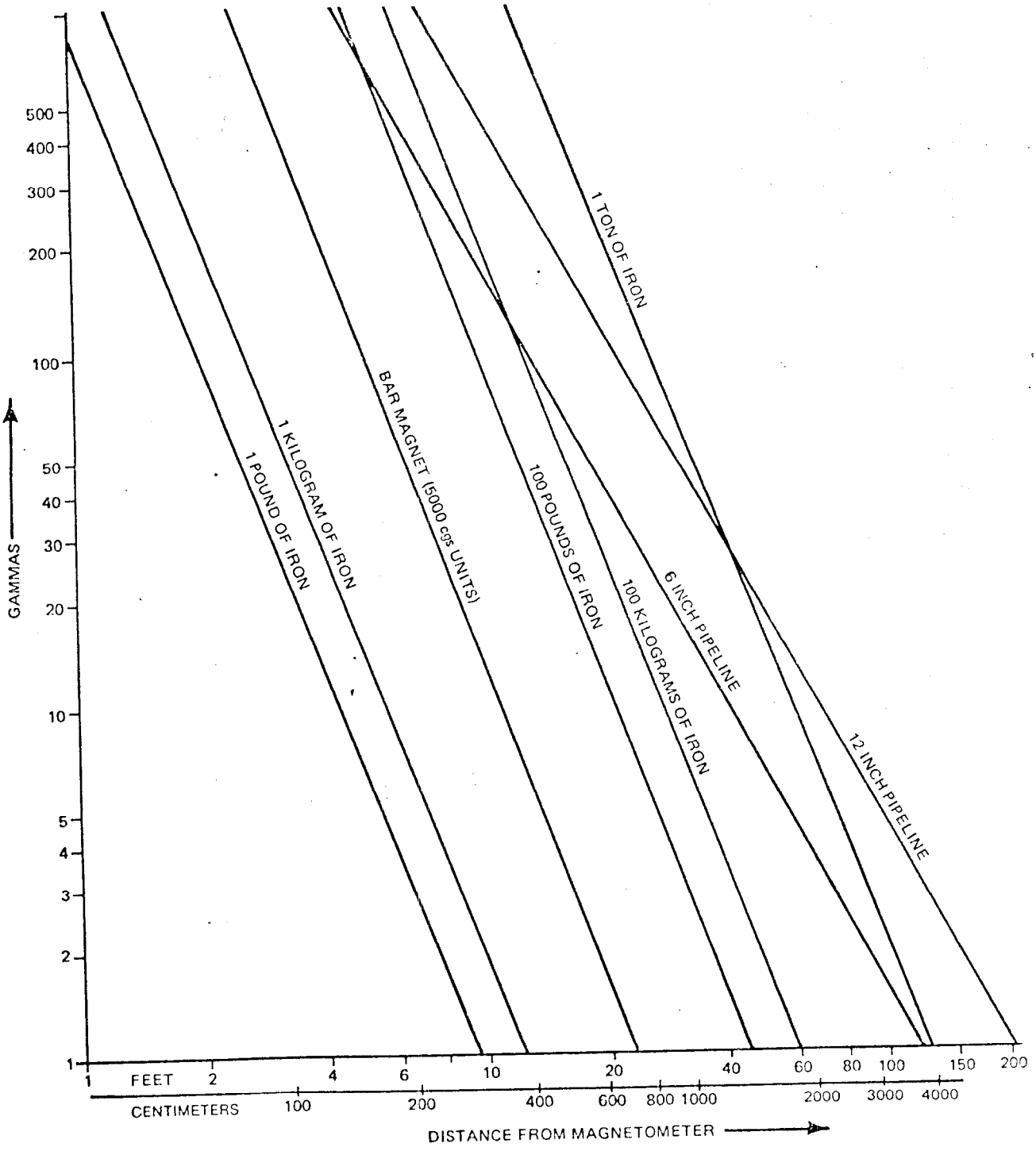

Figure 1. Nomogram for estimating magnetic anomalies.

Magnetometer surveys over rail lines do show magnetic anomalies of 1500 gammas relative to the background field when measured by the portable sensor eight feet above the surface of the ground. Figure 2 shows two parallel profiles normal to an east-west rail spur in Fort Belvoir, Virginia.

We ran a more elaborate survey of eight profiles over a rail spur in Alexandria, Virginia (see map on Figure 3). The anomalies over these profiles are shown on Figure 4. The interesting feature of these profiles normal to the rails is that they are not all of the same sign. Profiles run parallel to the rails as shown on Figure 5 demonstrate the oscillatory behavior of these anomalies. The half-wavelength of these oscillations correspond roughly to the length of the rails (33 feet). These anomalies are reproducible even when measured on different days as indicated by the x's on the center profile. It is as though one end of the rail is a north pole and the other a south pole.

The first magnetometer survey over a tunnel we conducted at the Carothers Tunnel on the main line of the B&O Railroad near Paw Paw, West Virginia. Figure 6 shows a photograph taken over the East Portal of the Carothers Tunnel. An operator is shown with the portable magnetometer and the sensor at the end of the 8 foot aluminum pole. Also shown are the telephone wires running over the tunnel. In many places these wires are less than 8 feet off the ground. Figure 7 shows a plan view of the railroad (which is double tracked), the east tunnel portal, the phone line, and several of the magnetometer profiles run over the tunnel. Figure 8 shows the magnetic field variations for two profiles over the rails at a scale of 1000 gammas per inch. The lowest magnetometer profiles over the tunnel are also plotted on the same figure with the same vertical scale.

Figure 9 shows the magnetometer profiles at the higher levels with a vertical scale of 20 gammas per centimeter. The position of the rails under each profile and the location of the phone line along each profile are clearly marked.

There is a distinct magnetic anomaly due to the phone line on each profile. There are other magnetic variations over the rail but it is difficult

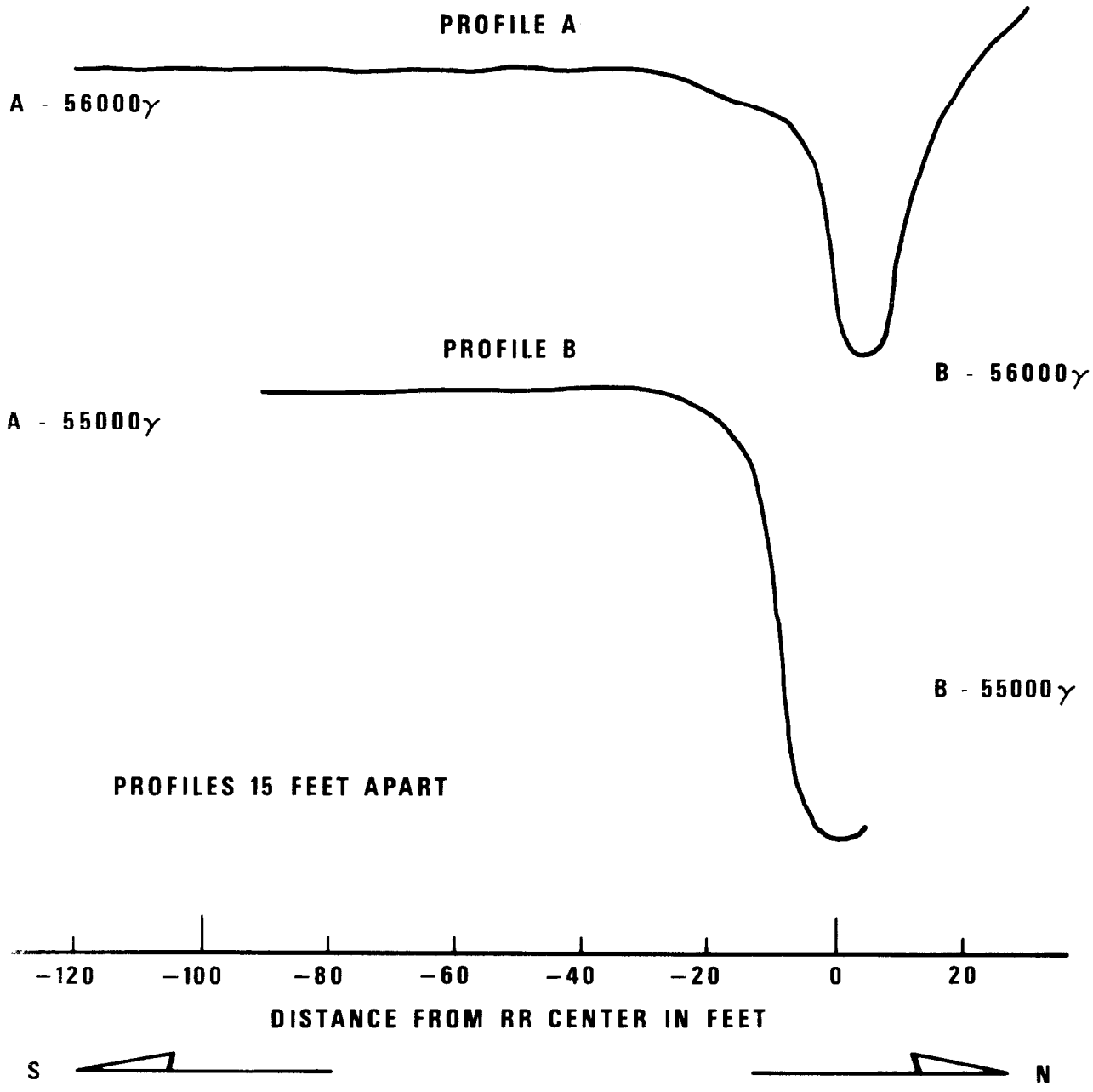

Figure 2. Magnetic survey over rail spur at Ft. Belvoir, Virginia.

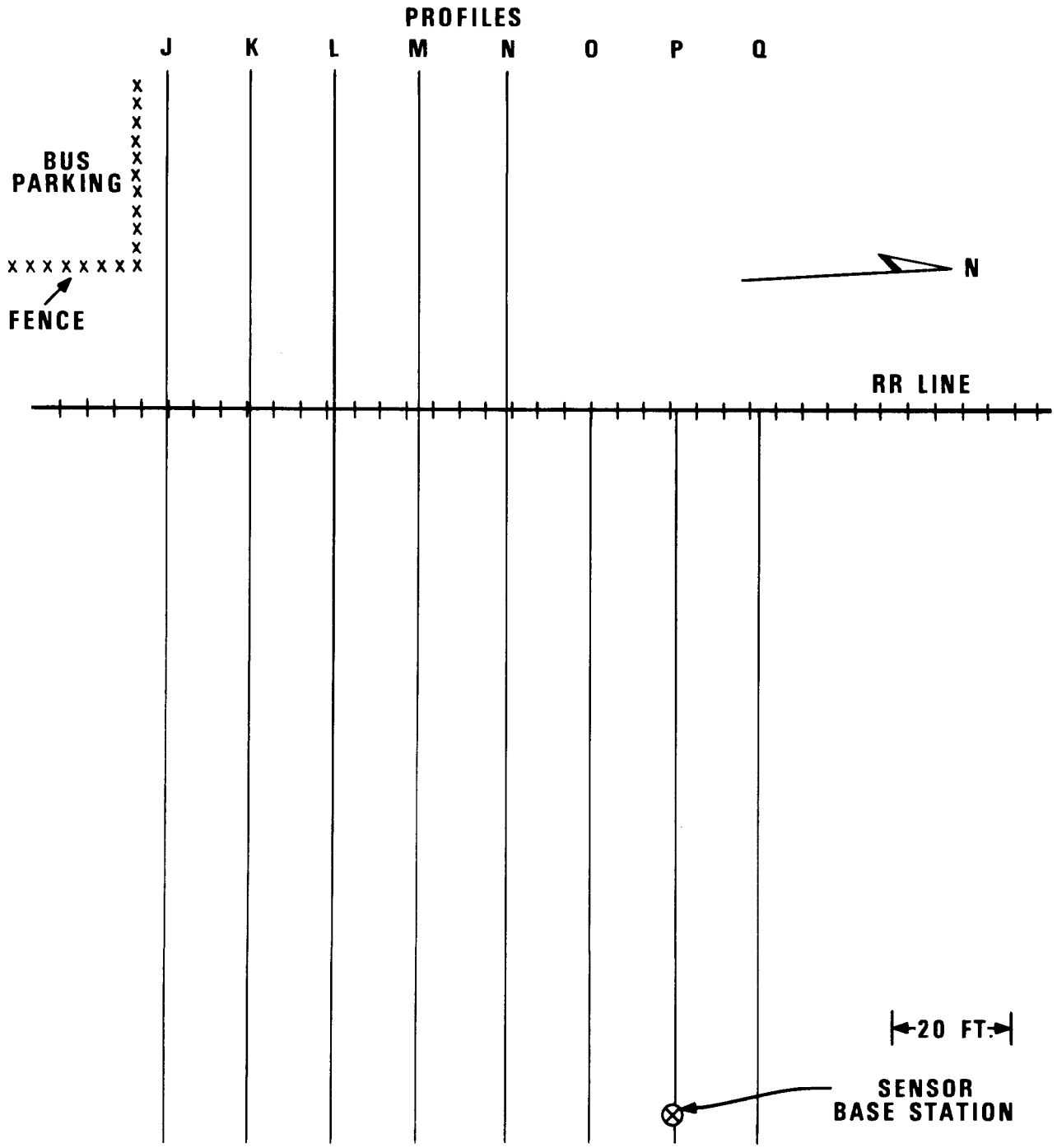

THE RR LINE IS ONE BLOCK EAST OF N. FAIRFAX ST., ALEXANDRIA, VA.
PROFILE M IS ON THE NORTH EDGE OF WYTHE ST., ALEXANDRIA .
PROFILE SEPARATION IS 15 FEET.
READINGS EVERY 1 FOOT FROM 0 TO 6 FEET FROM RR,
" 2 FEET " 6 TO 20 " " ",
" 5 FEET " 10 TO 100 " " ",
" 10 FEET " 100 TO 130 " " ".

Figure 3. Map of magnetic survey, Alexandria, Virginia.

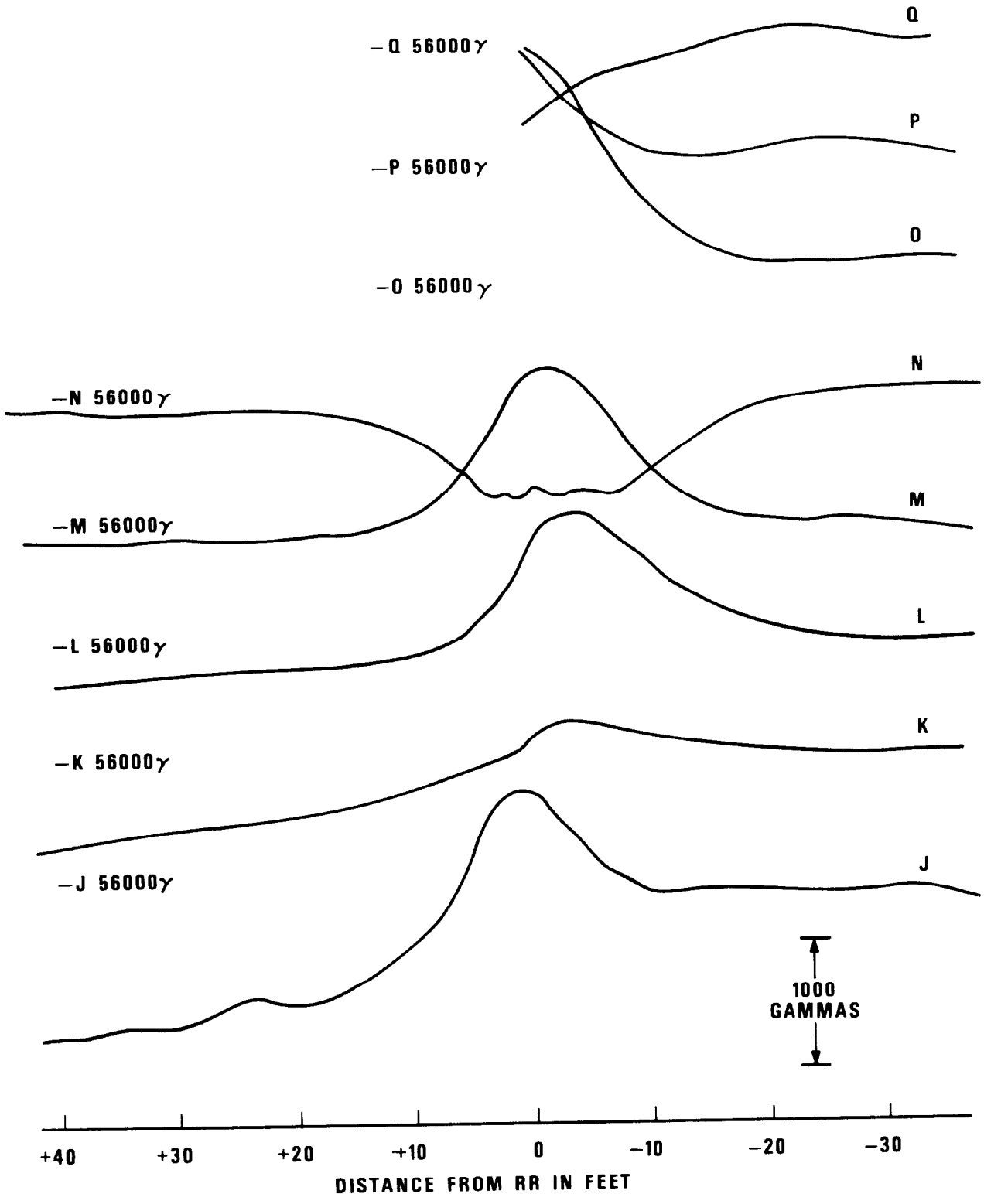

Figure 4. Magnetic survey over rail spur, Alexandria, Virginia.

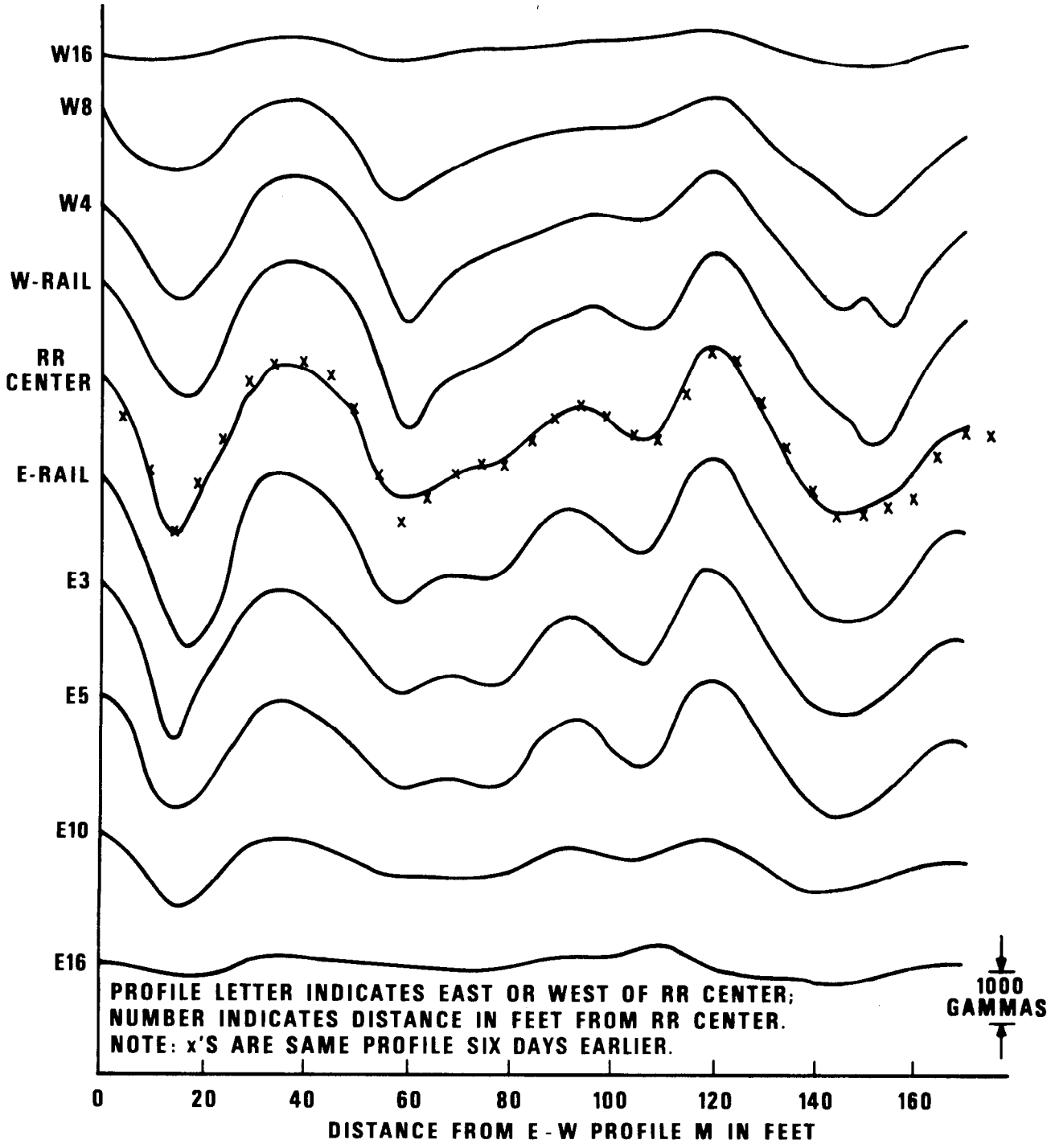

Figure 5. Magnetic profiles parallel to the rails, Alexandria, Virginia.

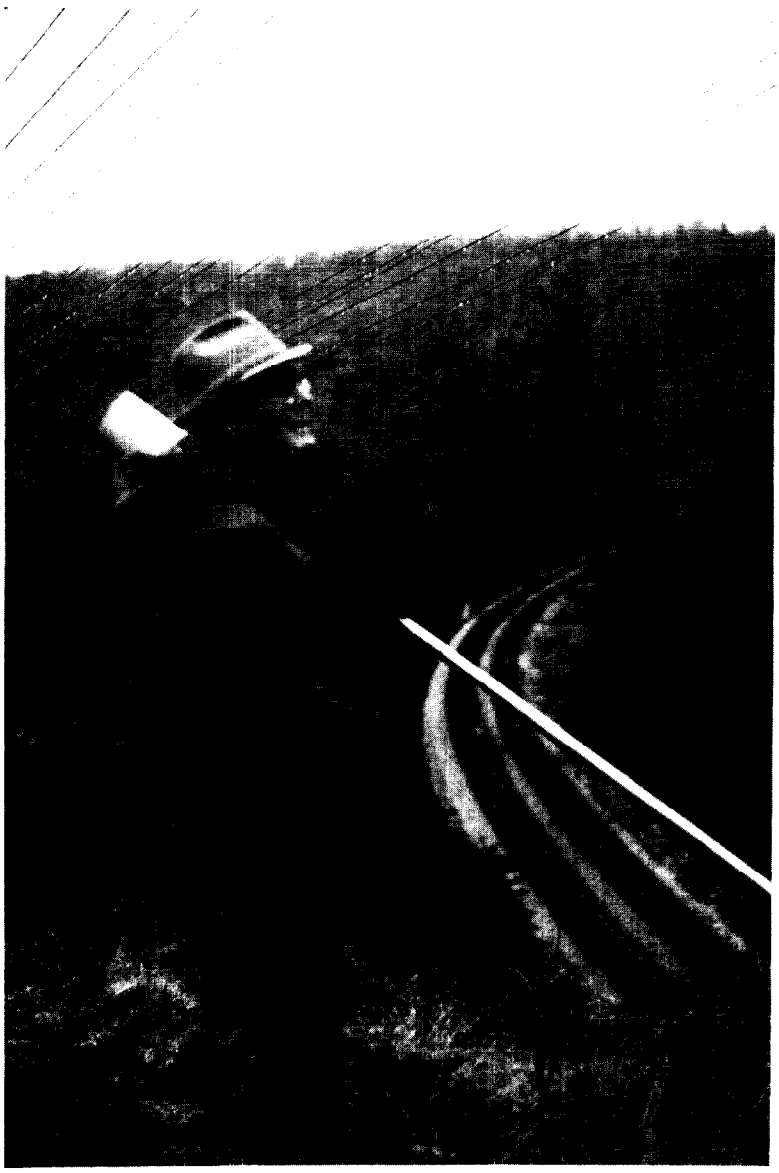

Figure 6. Operator with portable magnetometer over east portal, Carothers Tunnel, B&O Railroad.

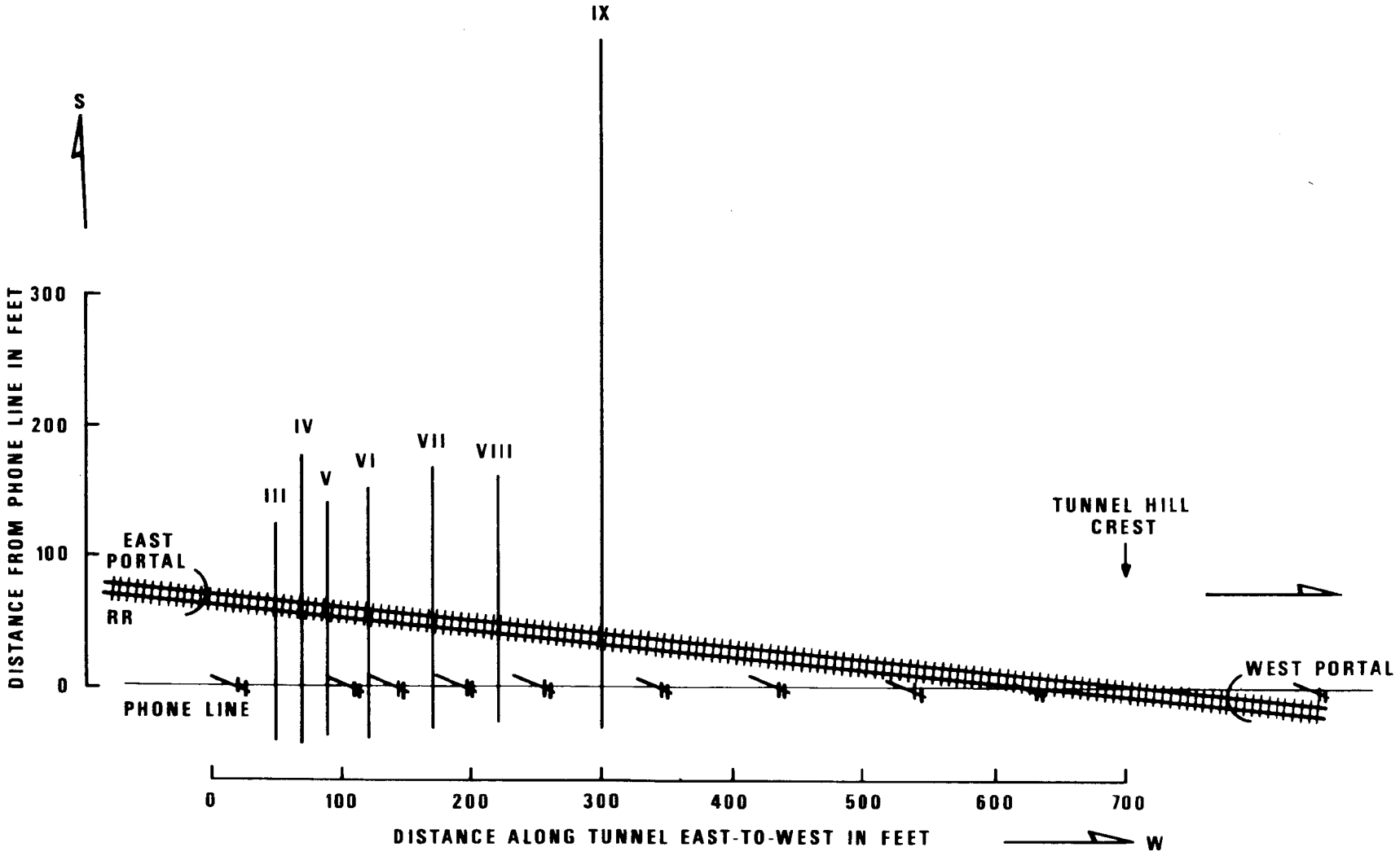

Figure 7. Map of magnetic survey over Carothers Tunnel, B&O Railroad.

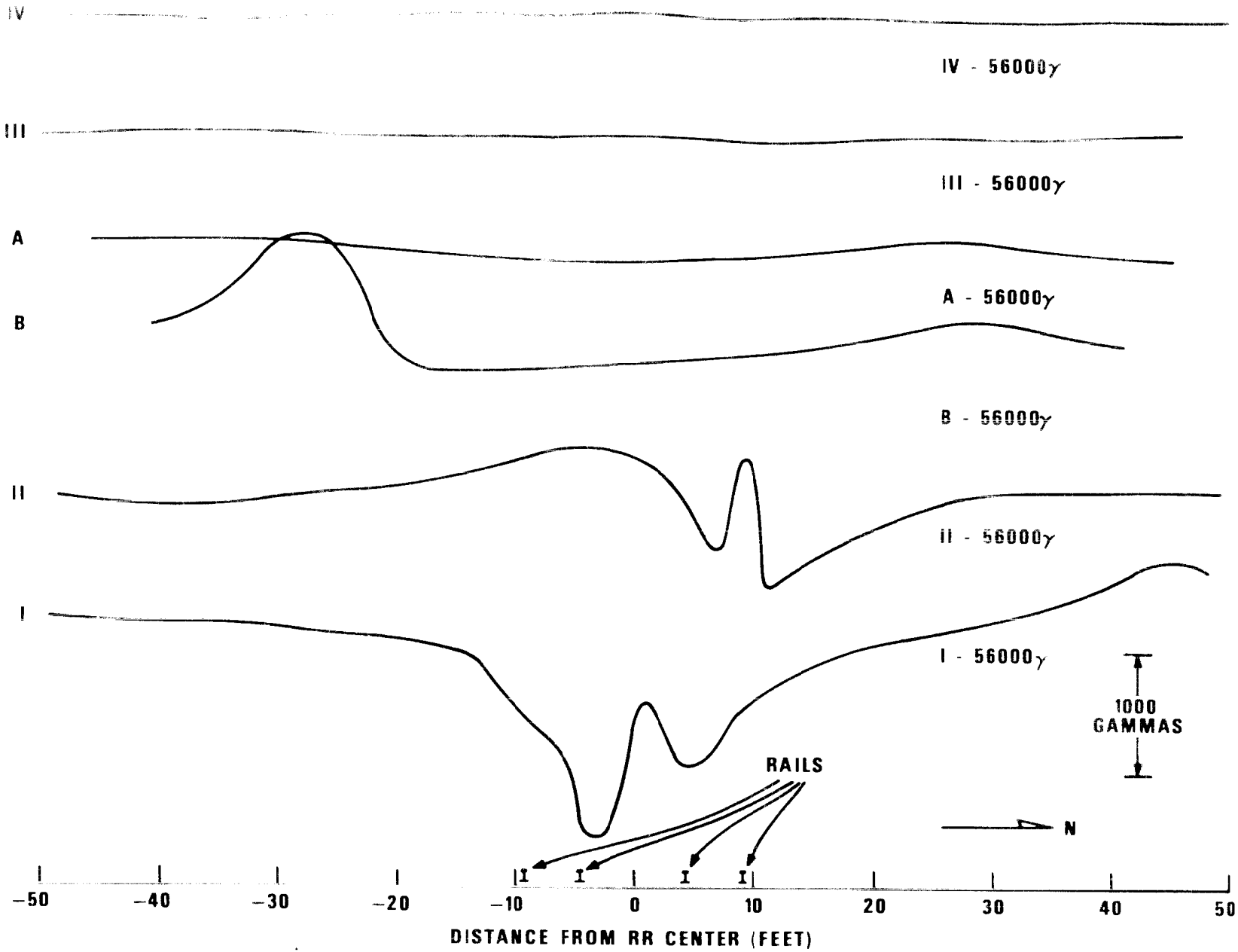

Figure 8. Magnetic anomalies over Carothers Tunnel, B&O Railroad.

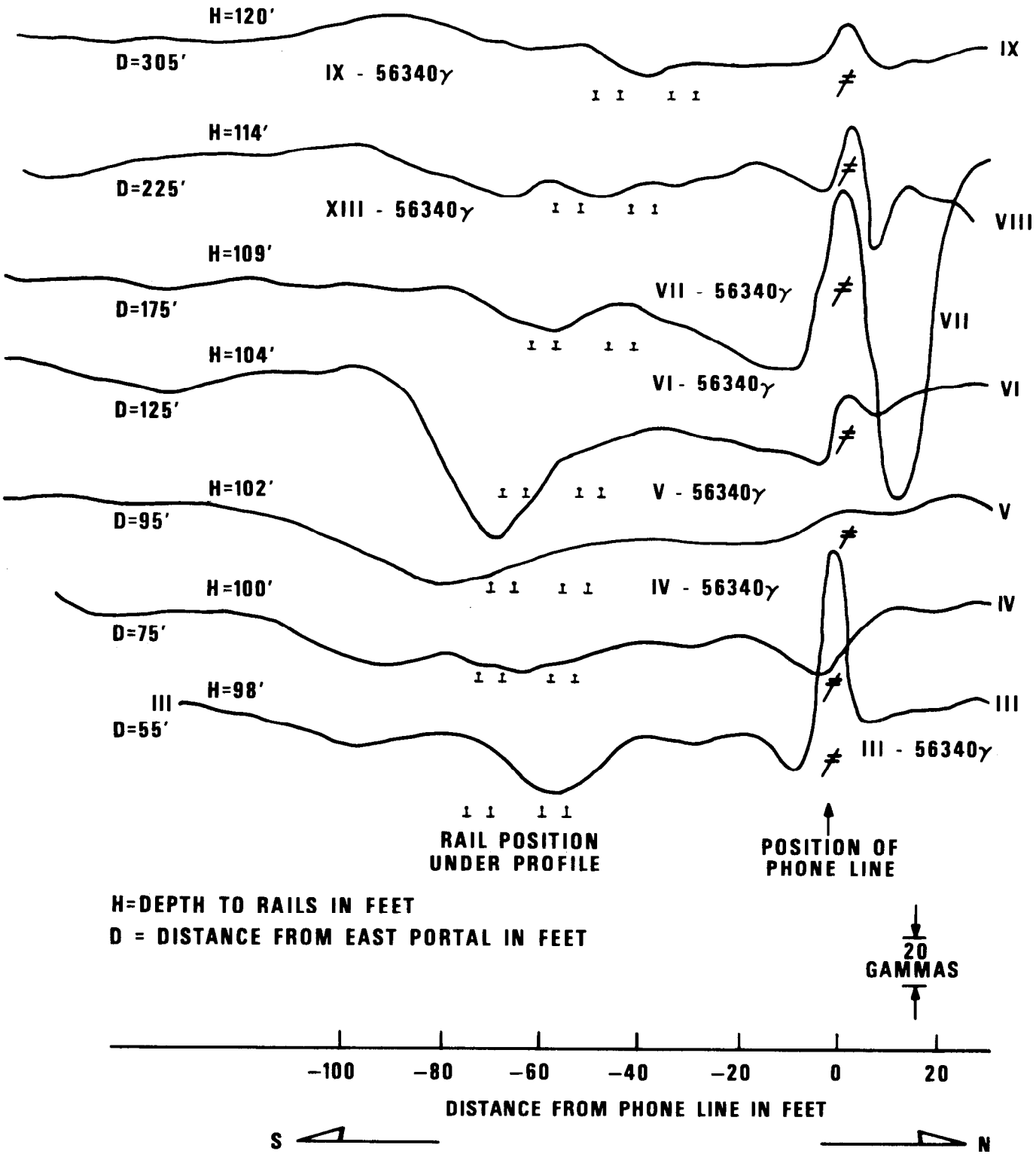

Figure 9. Magnetic survey, upper profiles, over Carothers Tunnel, B&O Railroad.

to attribute these variations directly to the rails, especially in light of the strange anomalies measured on the two parallel profiles directly over the rails (profiles I and II on Figure 8).

A more thorough magnetometer survey was run over Tunnel 19 of the Denver and Rio Grande Western Railroad near Eldorado Springs, Colorado. This tunnel (the west portal of which is shown in Figure 10) is in granite, has a single track, and has much easier access over the tunnel than the one in West Virginia. Figure 11 shows a map of the railroad, east portal of the tunnel, fences, phone lines, and the 21 profiles run. Figure 12 shows a cross section of the tunnel and the profile elevations along the phone line. Profile A is 50 feet and profile U is 90 feet above the rails. Figure 13 shows an operator with a portable magnetometer at the upper profiles over Tunnel 19.

We conducted a track level survey as well. The railroad crosses a high fill immediately east of Tunnel 19 which provides only limited access to the north and south of the rails. Figure 14 shows the magnetic anomalies over the north rail and 10 feet to the north, and over the south rail and 10 feet to the south. Again the oscillatory character of the magnetic anomalies is evident and again the oscillation half-wavelength corresponds roughly to the rail length of 39 feet.

The magnetic data for the 21 profiles over the tunnel are shown in Figure 15. As was consistent with most of our surveys magnetometer readings were taken every 5 feet along the north-south profiles. The profile spacing, east to west, was 8.5 feet. A base station magnetometer was recording at the top of the mountain 140 feet above the rails. A constant base station correction was applied to each half profile (i.e. to those readings taken within 10 minutes of each other).

The magnetic profiles show strong fence and phone line anomalies. Since they are parallel to the rails, their strong anomalies tend to obscure the weaker ones which might be expected from the rails.

Figure 10. West portal of Tunnel 19, DRGW Railroad.

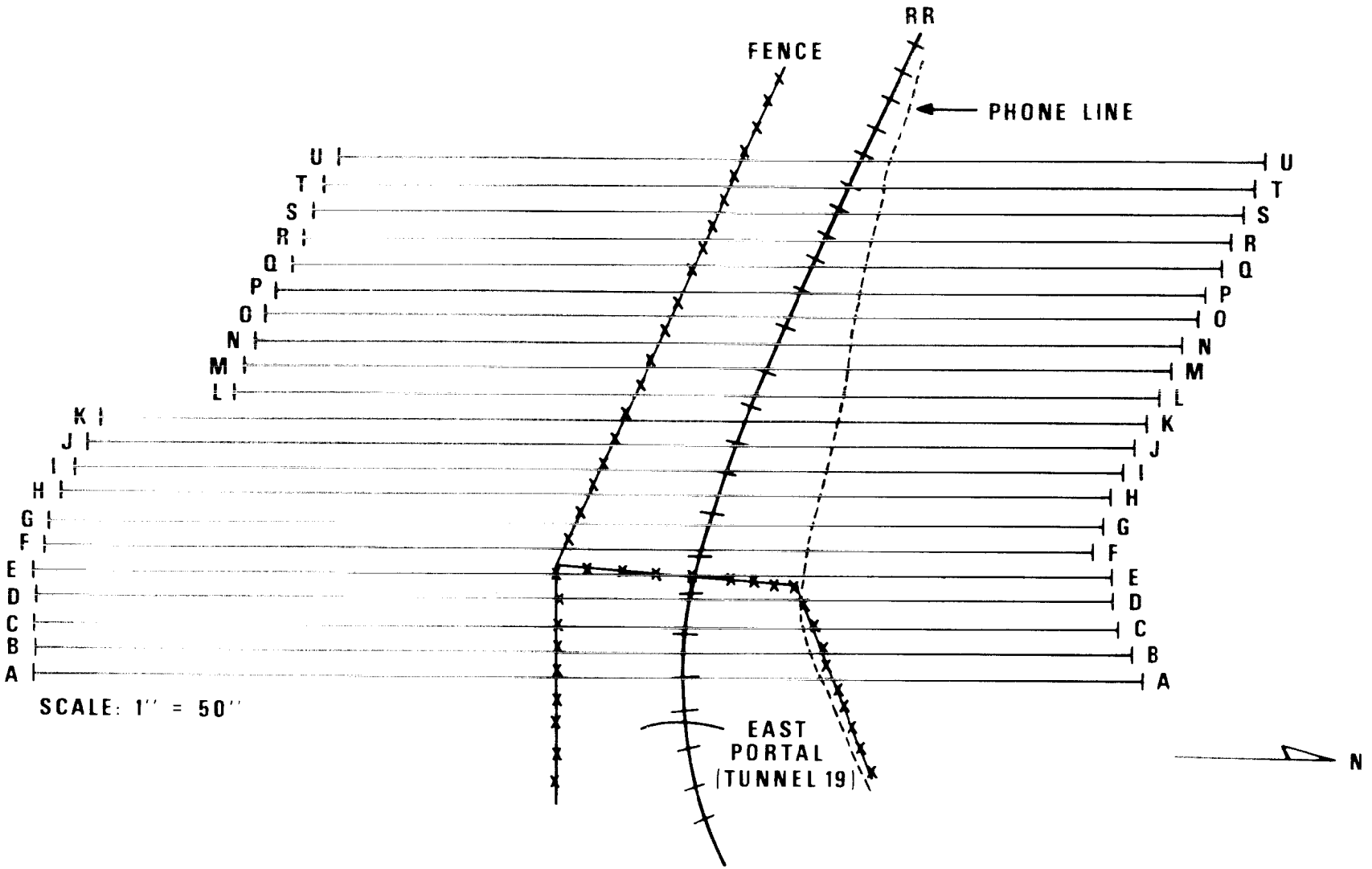

Figure 11. Map of magnetic survey over Tunnel 19, DRGW Railroad.

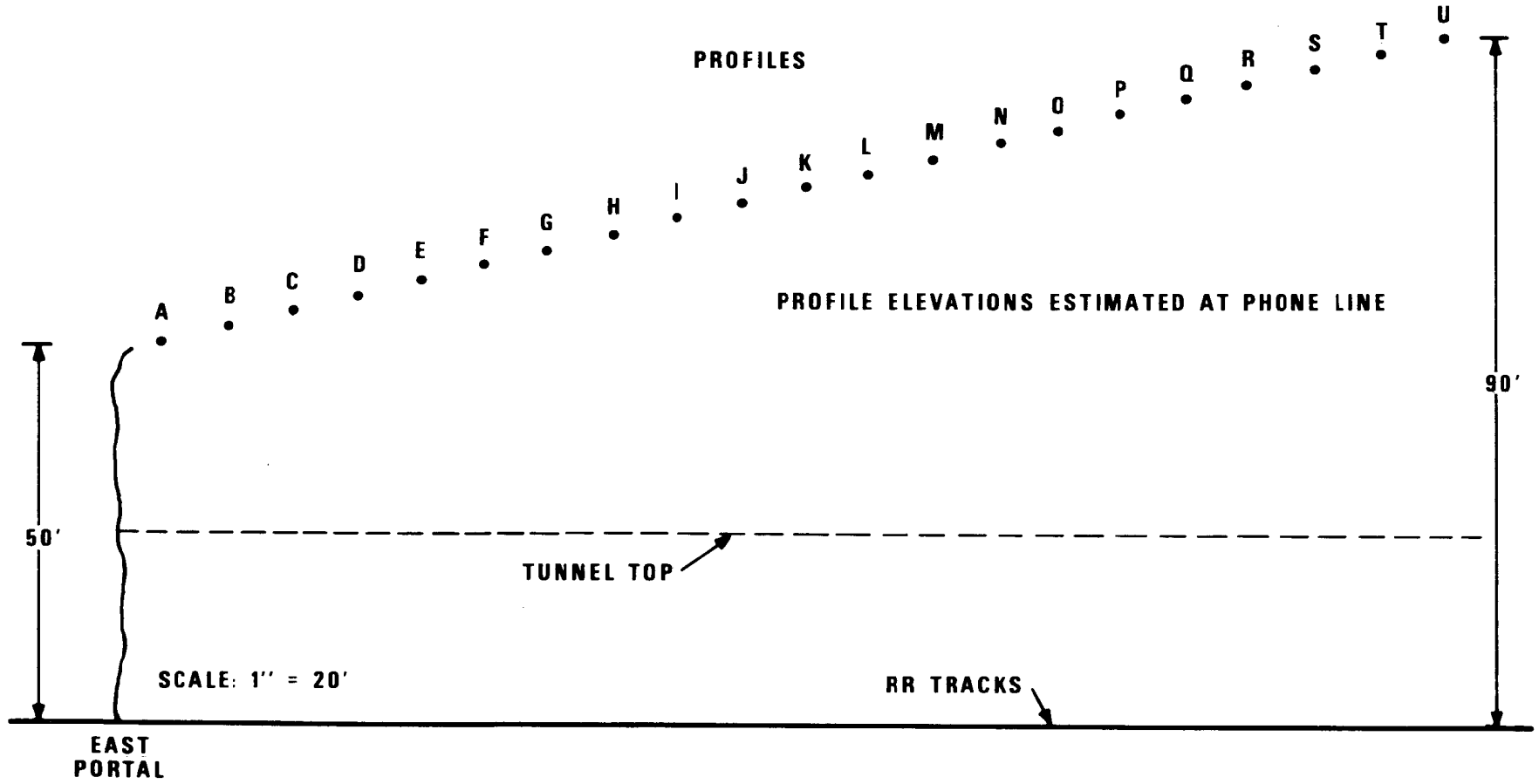

Figure 12. Cross section of Tunnel 19 and magnetic profiles, DRGW Railroad.

Figure 13. Operator with portable magnetometer of upper profiles over Tunnel 19, DRGW Railroad.

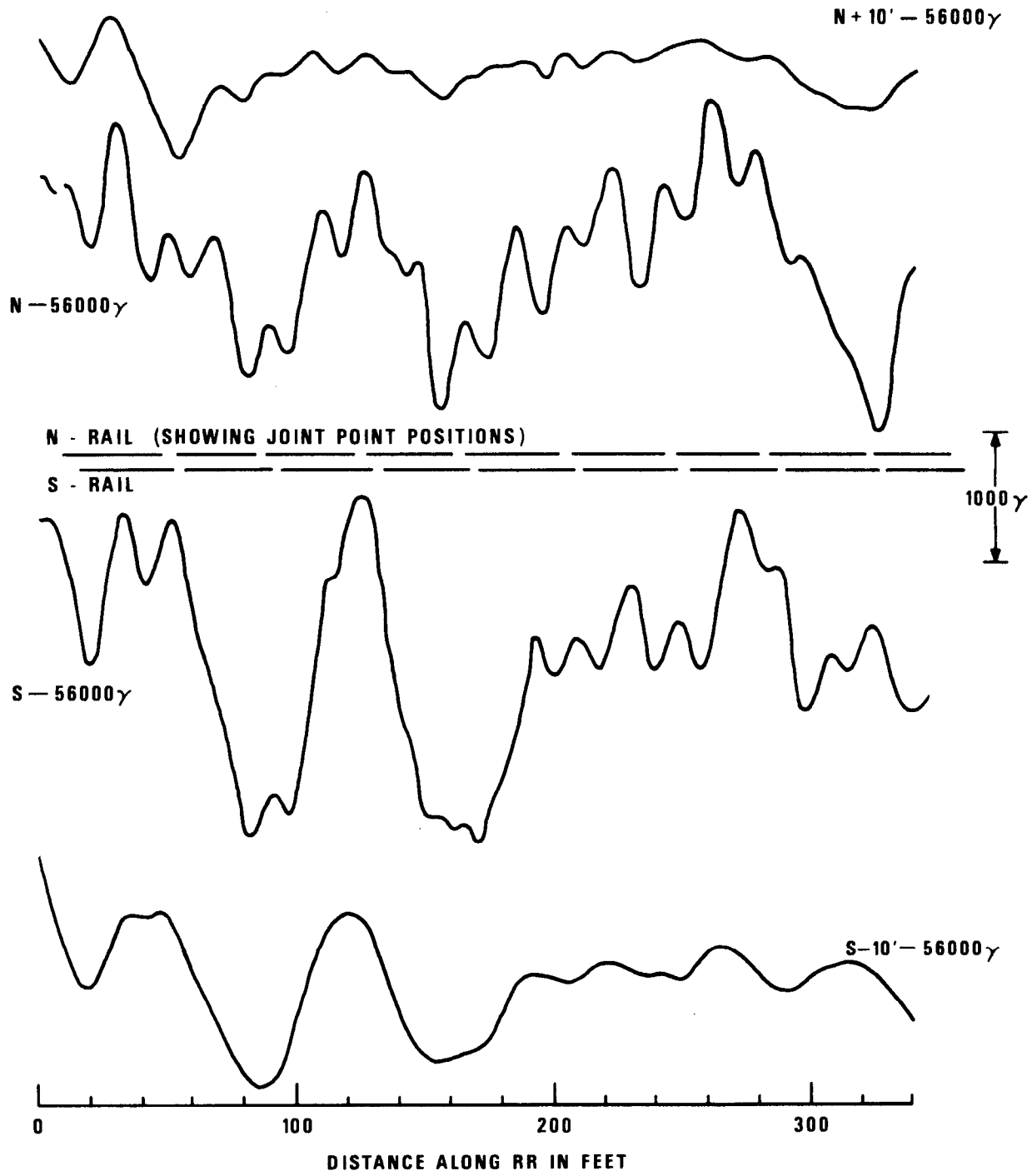

Figure 14. Trackside magnetic survey near Tunnel 19, DRGW Railroad.

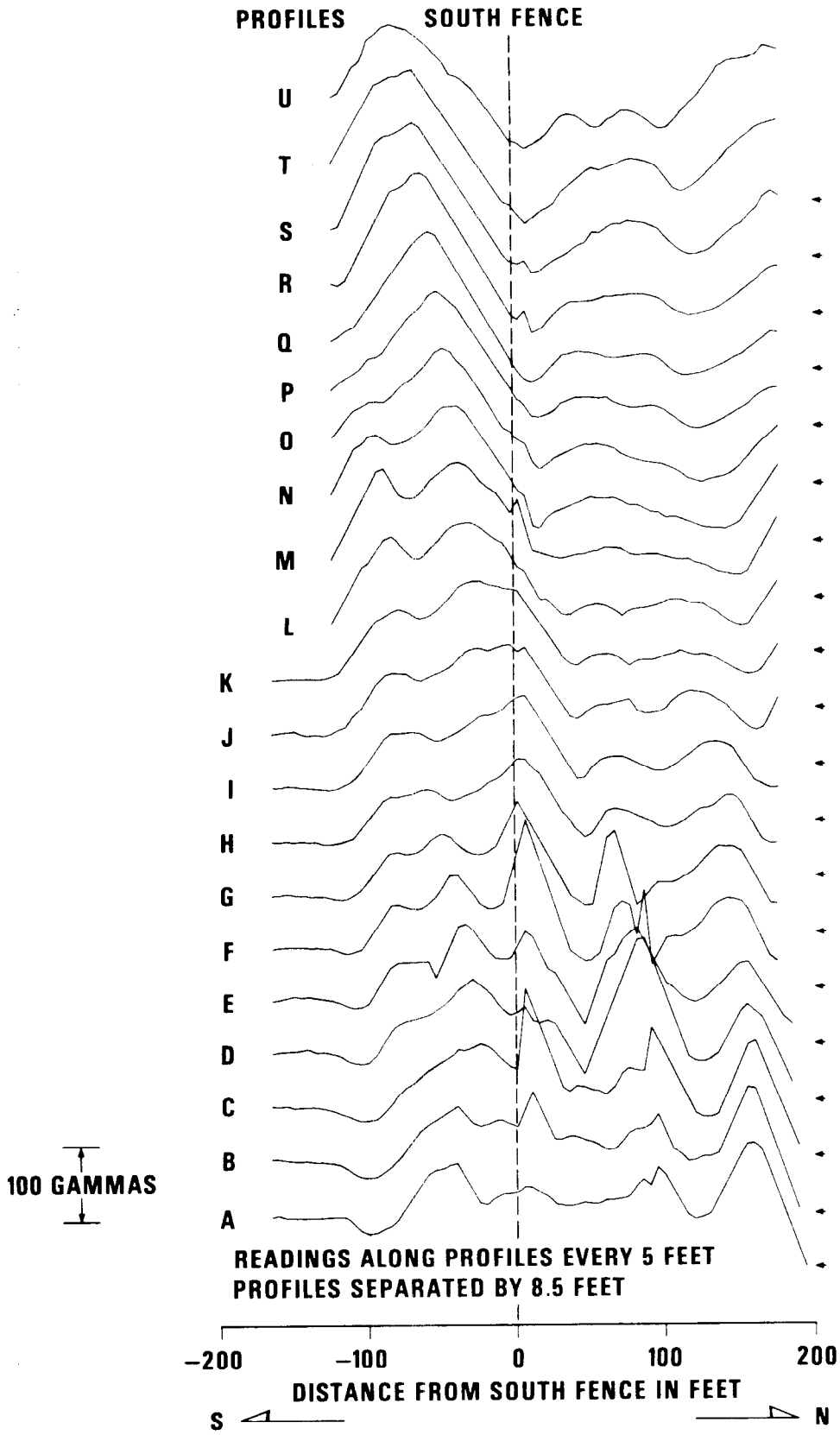

Figure 15. Magnetic survey over Tunnel 19, DRGW Railroad.

We applied several kinds of smoothing. First we smoothed out the fence and phone line anomalies by hand. We also made a computer interpolation for each profile as follows:

$$\text{Profile A} = \sum_{k=-N}^{+N} a_k \frac{\sin(x-k\Delta x)\pi/\Delta x}{(x-k\Delta x)\pi/\Delta x} .$$

Trends were removed first to avoid the Gibbs effect at the ends which would otherwise be discontinuities. These smoothed data are plotted in Figure 16.

We can estimate the rail anomalies at each of the over-tunnel profiles from a theoretical argument. If the anomalies at rail level vary sinusoidally, and vary inversely as the square of the rail-magnetometer separation, then to a first order approximation, the rail magnetic anomalies should be:

$$\phi(x,y) = \frac{M_o}{h^2 + x^2} \cos \frac{\pi y}{L} \qquad (1)$$

where h is the height of the sensor above the rails, x is the distance along the profile in a north-south direction from the rail center, and y is the distance in the east-west direction from Profile A. The half-wavelength L, is equal to the rail length. Figure 17 shows the expected anomalies from the rails at each of the profiles over the tunnel plotted to the same scale of the measured data on Figures 15 and 16. Since the rail anomalies are small, broad and oscillatory, they are readily obscurred by the larger, sharper, and more continuous geologic anomalies and especially the larger and sharper phone line and fence anomalies running parallel to the rails.

Since it is the oscillatory behavior of the rail anomalies which most effectively hides them in the geologic anomalies, we can ask whether some other measure of the magnetic field would give an effect more constant in value along the axis of the rails. One possiblity is the gradient. The magnetometer measures the vector sum of the earth's field and that from the rails. Thus the effect from the rails could be a rotating vector rather than one that goes to zero. If the form of the rail anomaly is given by equation (1), then the gradient will be:

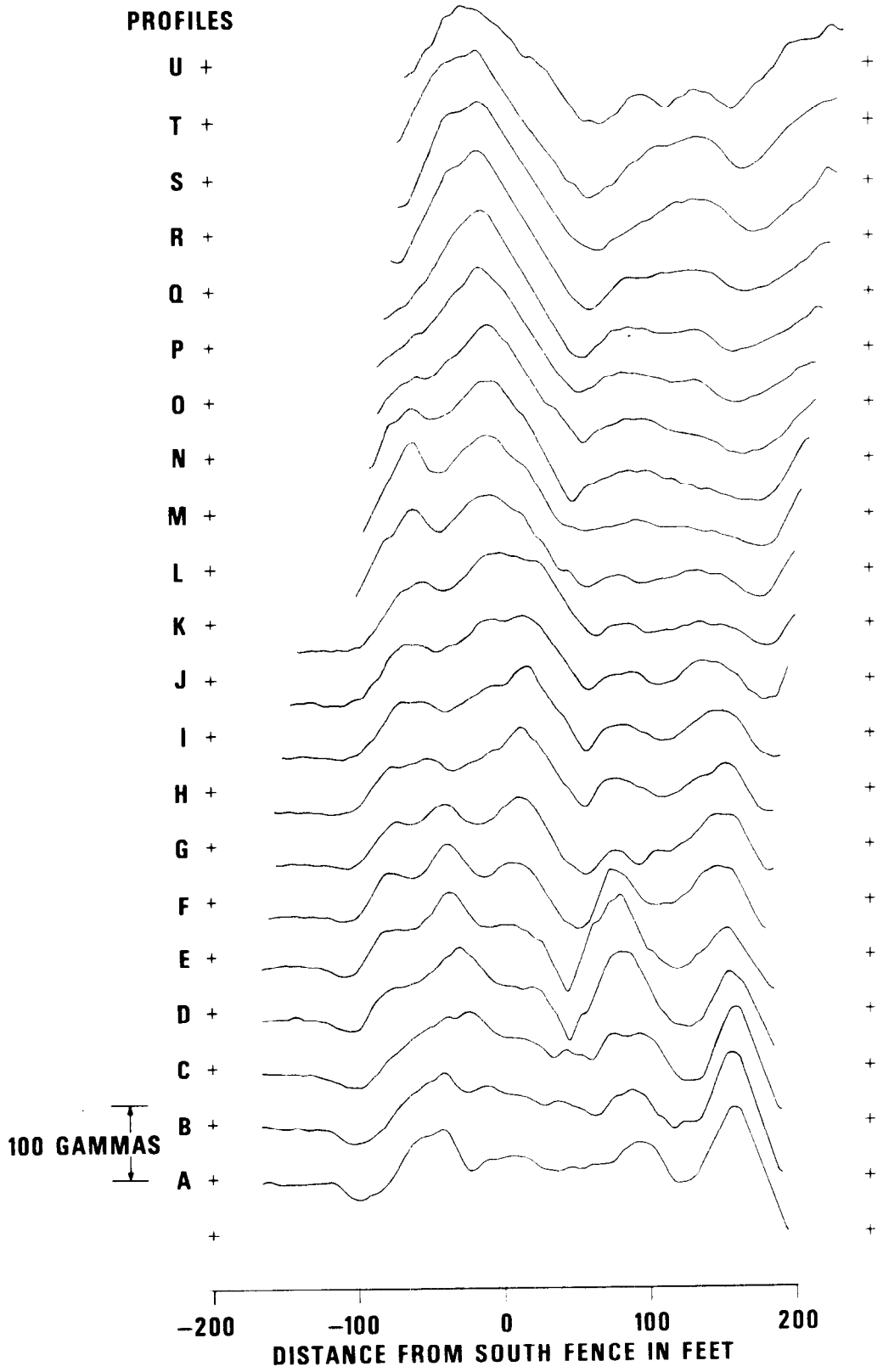

Figure 16. Smoothed magnetic profiles over Tunnel 19, DRGW Railroad.

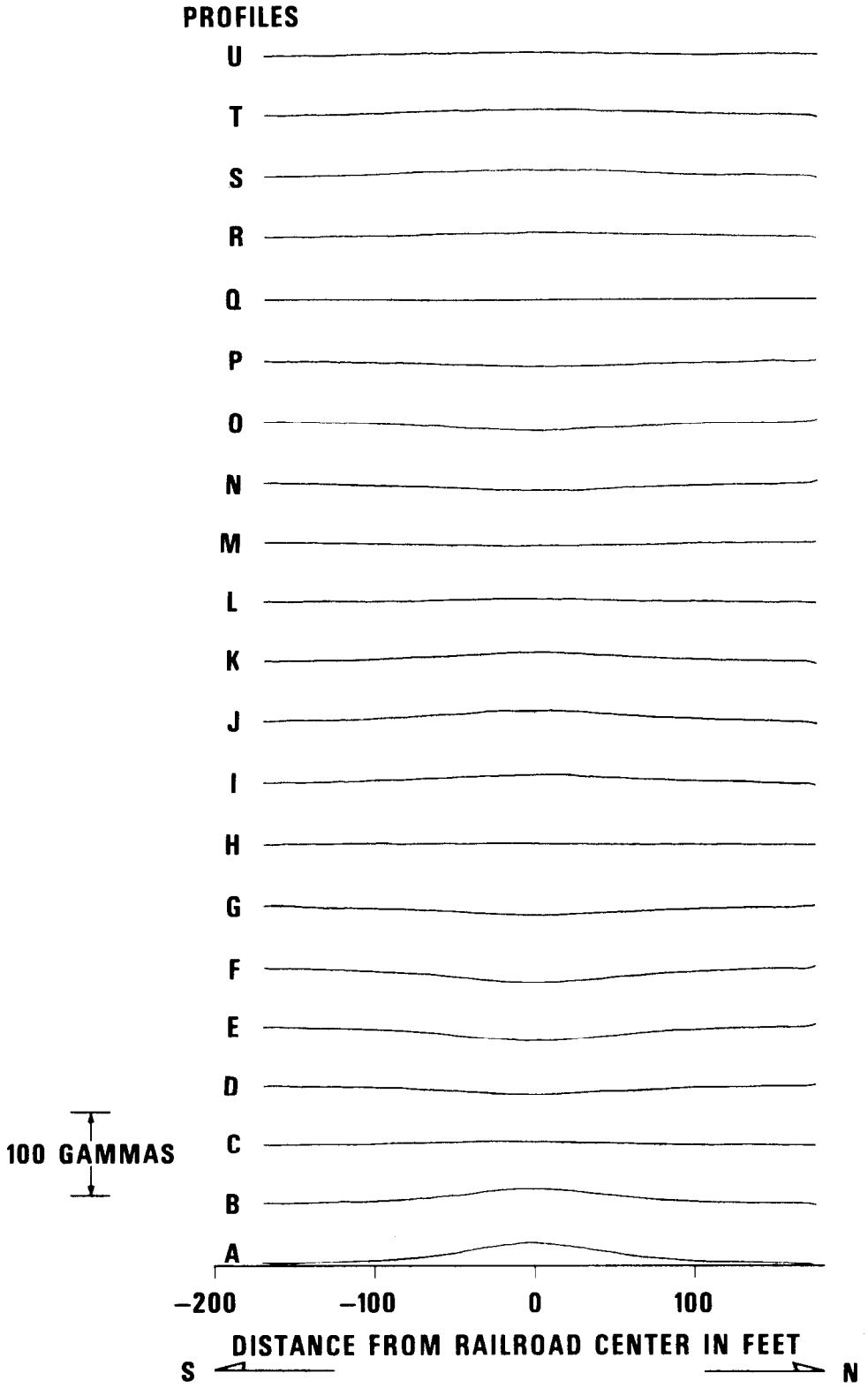

Figure 17. Expected anomalies from rails over Tunnel 19, DRGW Railroad.

$$\nabla\phi(x,y) = i\,\frac{\partial\phi}{\partial x} + j\,\frac{\partial\phi}{\partial y} \qquad (2)$$

$$= \frac{M_o}{h^2 + x^2} \; -i\,\frac{2x}{h^2 + x^2}\cos\frac{\pi y}{L} - j\,\frac{\pi}{L}\sin\frac{\pi y}{L} \quad .$$

The absolute value of the gradient will be

$$|\nabla\phi| = \frac{M_o}{h^2 + x^2}\left[\frac{2x}{h^2 + x^2}\right]^2 \cos^2\frac{\pi y}{L} + \left[\frac{\pi}{L}\right]^2 \sin^2\frac{\pi y}{L}\Bigg]^{1/2} .$$

In this form when

$$\frac{2x}{h^2 + x^2} = \frac{\pi}{L}$$

or when $x = +\frac{L}{\pi} \pm \left[\frac{L}{\pi}\right]^2 - h^2\Big]^{1/2}$

the coefficients of the sine and cosine terms are equal and the sinusodial variation of the absolute value of the gradient, ($|\nabla\phi|$), disappears.

To test whether empirical data yields reasonable values for h and L, we consider profile M from the Alexandria survey shown in Figure 18. The theoretical curve gives the fits the data approximately when h = 6.5 feet, a fairly close match to the sensor height of 8 feet, and L = 21 feet (found by averaging distances between zero crossings), which is the same order of the rail length (33 feet).

A theoretical gradient computed for the 21 profiles over Tunnel 19 of the DRG-RR is shown in Figure 19. Here the height, h, is the sensor height over the rails and rail length (L) is 39 feet.

The actual gradient of the data over Tunnel 19 with the phone line and fence anomalies smoothed out is shown on Figure 20. As shown on Figure 19 the expected gradient is still oscillatory as was the original field. Moreover, the gradient of the actual data does not show an anomaly trend parallel with the rails which can be readily attributed to the rails.

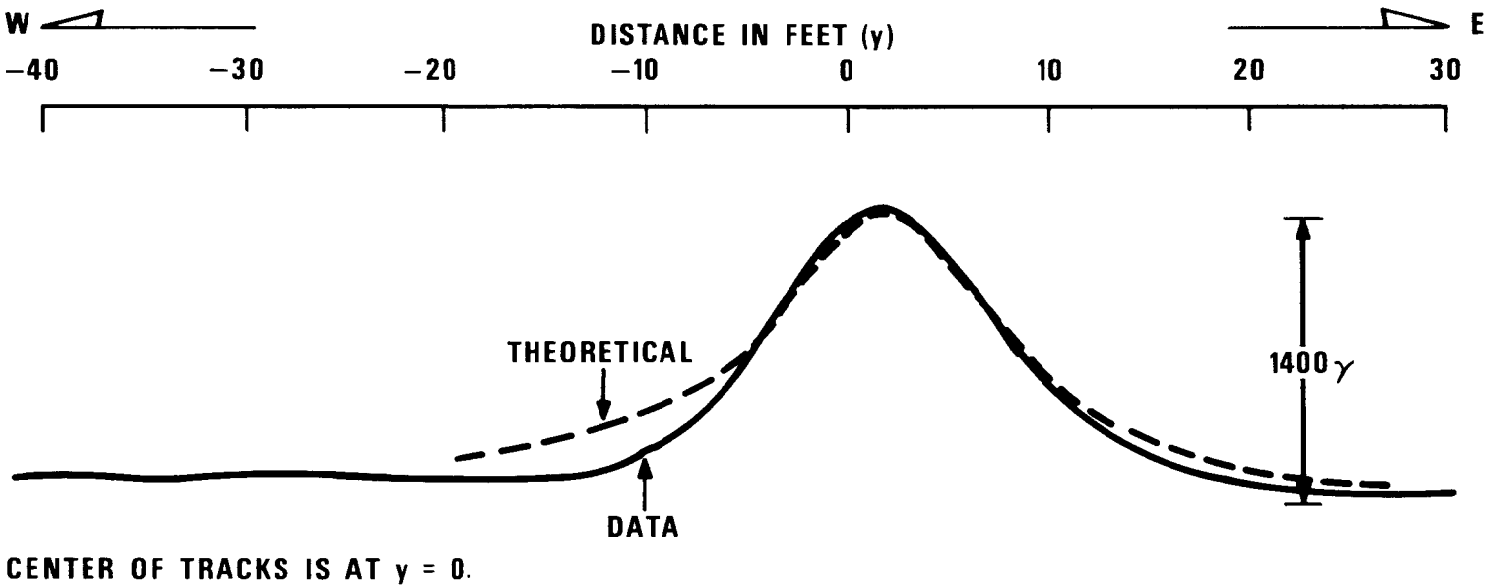

Figure 18. Actual versus theoretical anomaly, profile M, Alexandria survey.

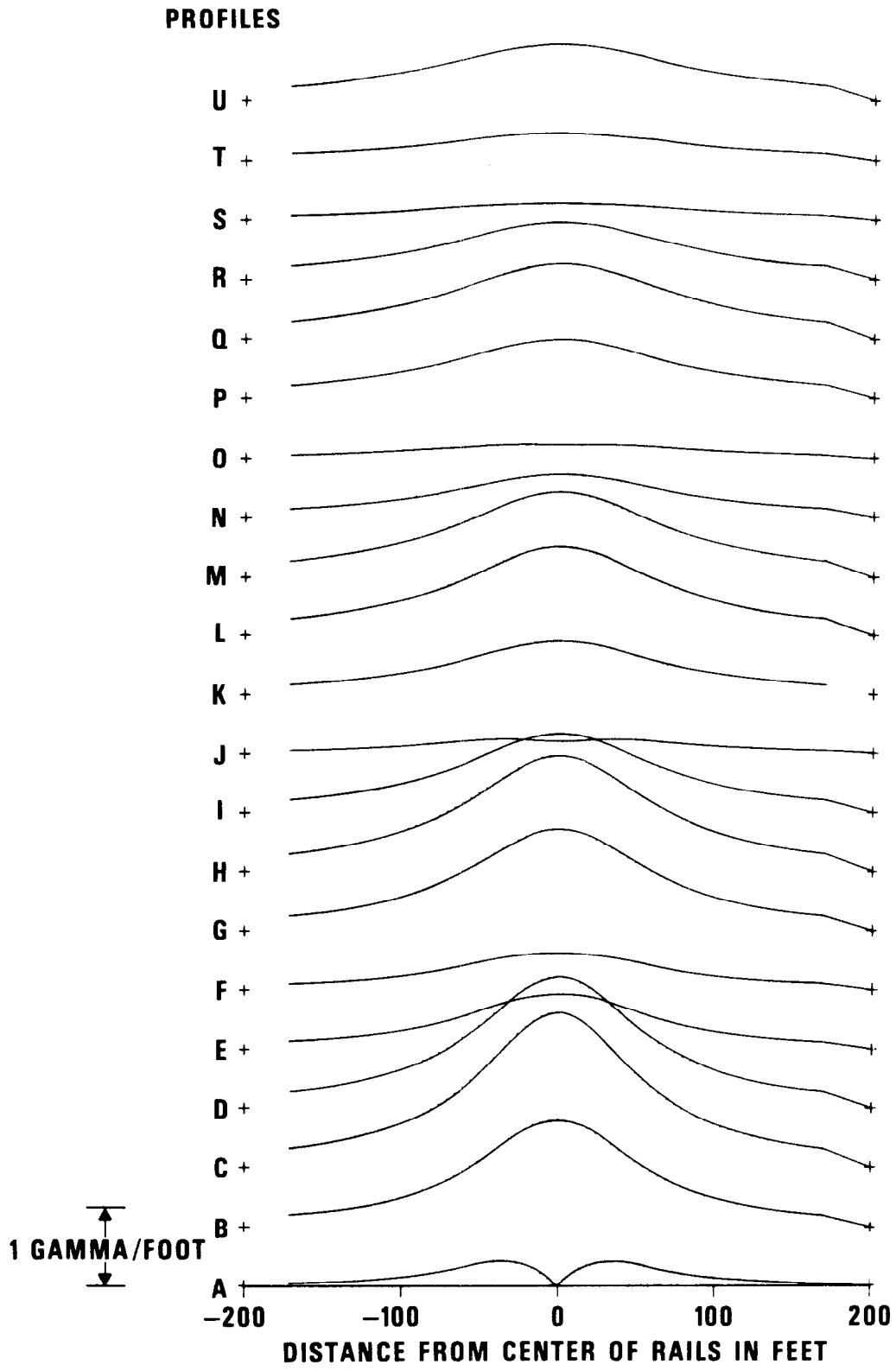

Figure 19. Theoretical gradient for 21 profiles over Tunnel 19, DRGW Railroad.

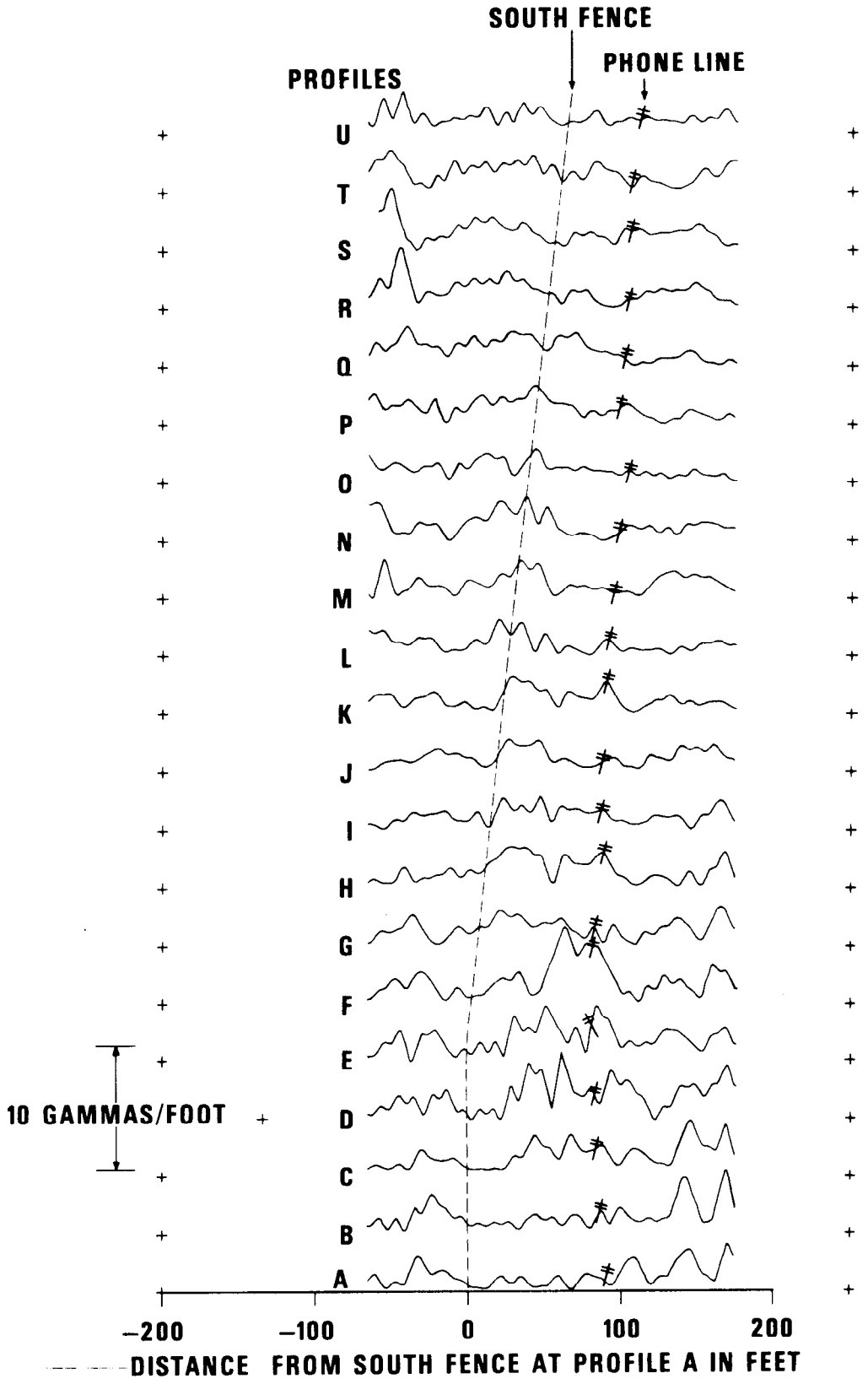

Figure 20. Actual gradient for 21 profiles over Tunnel 19, DRGW Railroad.

One type of magnetic anomalies is easy to detect. When a train is moving through the tunnel, erratic readings of several hundred gamma are easily detected on a magnetometer. Figure 21 shows a time series of such readings taken 10 seconds apart. This behavior is always apparent even when the sensor is 150 feet above the rails. Similar changes (20 to 100 gamma) in the background magnetic field were noticed when busses were parked or removed from a lot 100 feet from the base station during the Alexandria survey. Heavy equipment moving through a mine might be expected to have a similar effect.

The final test was a borehole magnetic survey conducted at the experimental mine of the Colorado School of Mines near Idaho Springs, Colorado. Geometrics built a special sensor for borehole use. It has a 2.5 inch outside diameter and is approximately two feet in length. It is hermetically sealed to a 600 foot cable. Figure 22 shows a photograph of the special sensor. Because of the extra length of the cable the base station magnetometer with a higher current capacity than the portable unit, must be used to drive the sensor.

Geometrics reports that this special sensor is not as good in cancelling stray electric fields as their standard sensor (4.5 inch outside diameter). However, we noticed no difference in the response of the sensor when the mine lights were on or off during our borehole tests.

We drilled a 34 foot borehole some 30 feet from the entrance of the CSM experimental mine. Figure 23 shows a photograph of the entrance to the experimental mine for the drilling operation underway over the mine. A map and cross sectional view is shown on Figure 24. The borehole was in granite and passed within 12 feet of the edge of the mine. The borehole was 15 feet from the center of the rails at its closest point.

We ran a survey over the rails outside the CSM Mine with the portable magnetometer. Figure 25 shows the magnetic profile along the rails. These mine rails weigh 28 pounds per yard. The rail anomalies measure 1000 gamma above the background field.

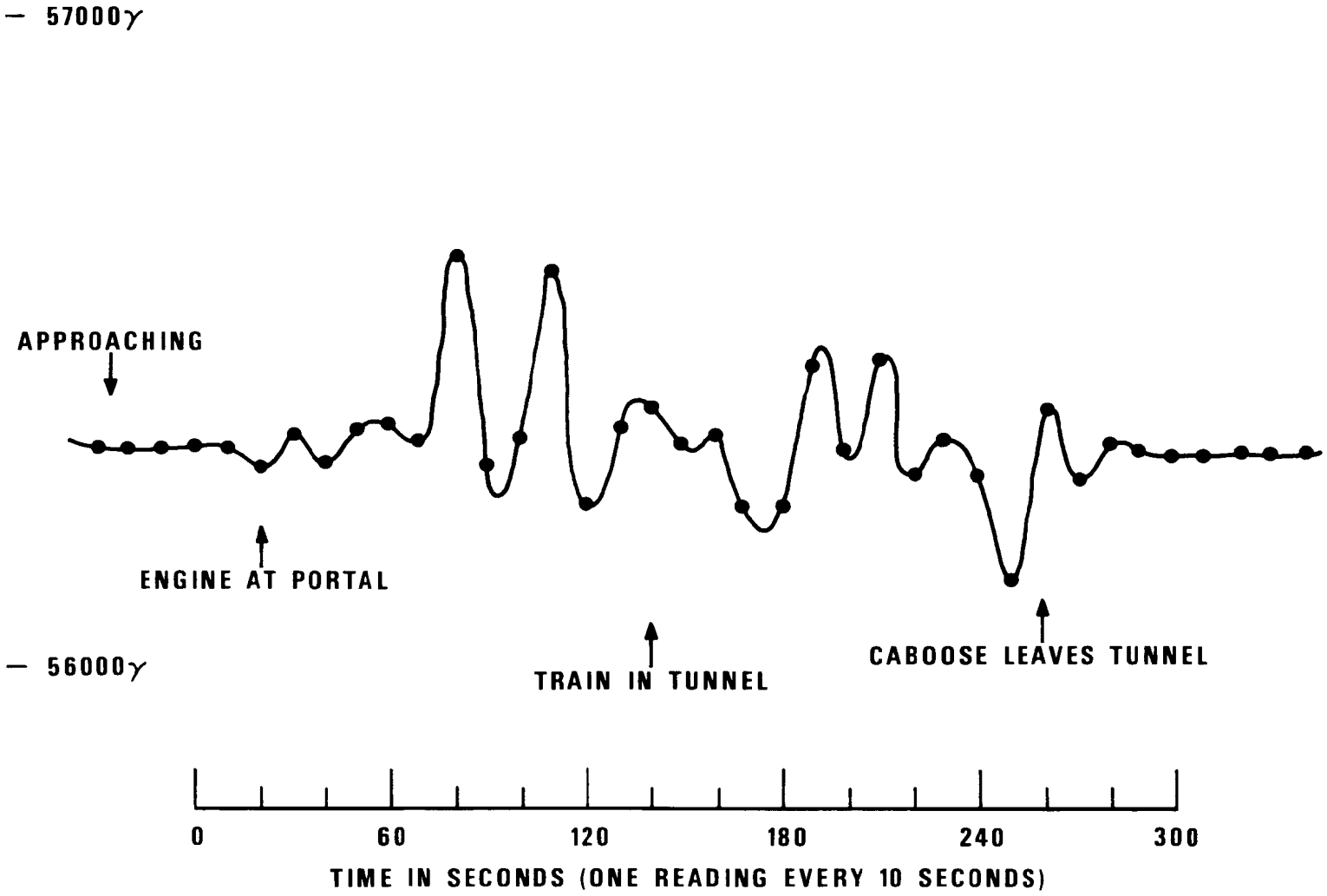

Figure 21. Magnetic anomalies from freight train passing through Carothers Tunnel, B&O Railroad.

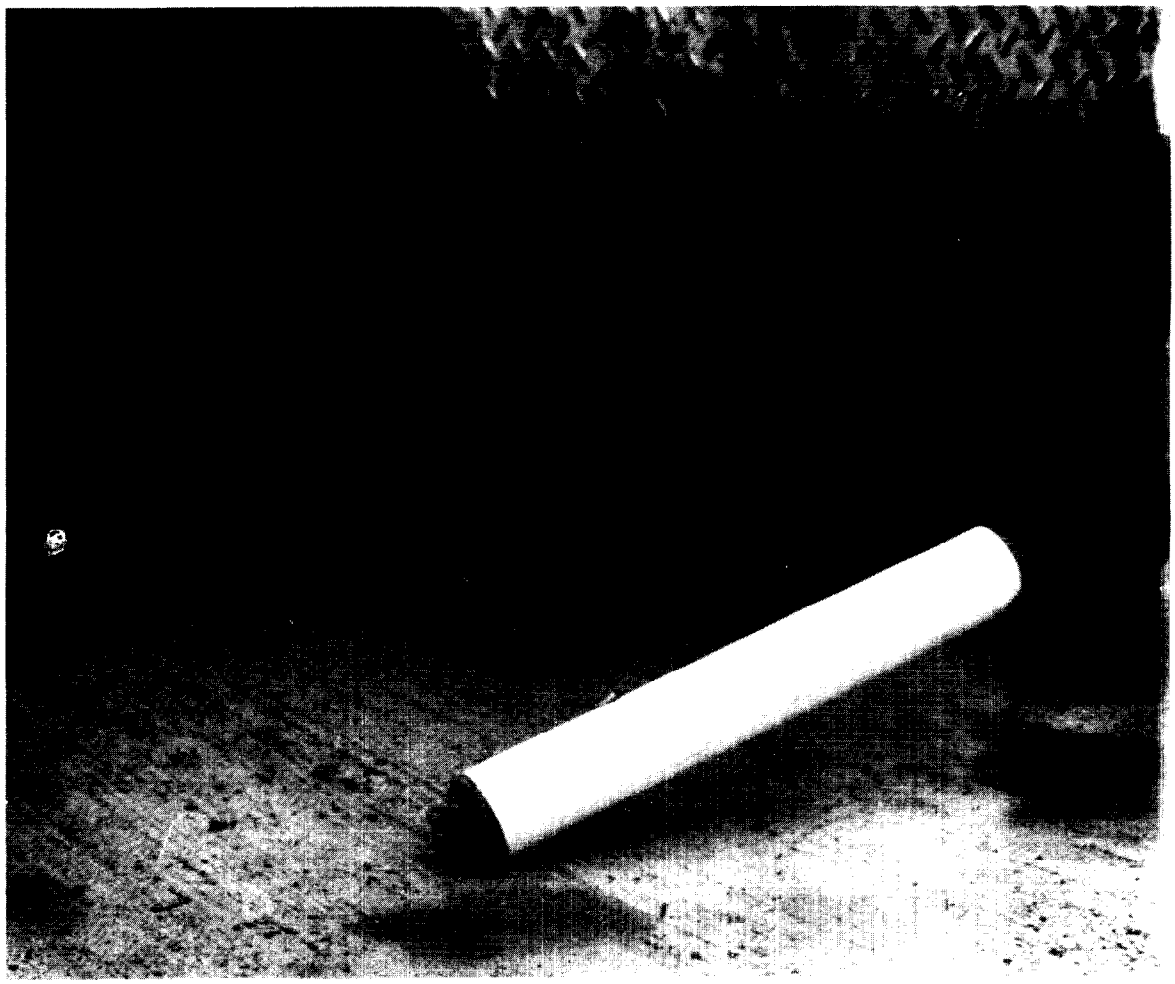

Figure 22. Special sensor for borehole magnetometer.

Figure 23. Drilling rig over Colorado School of Mines experimental mine.

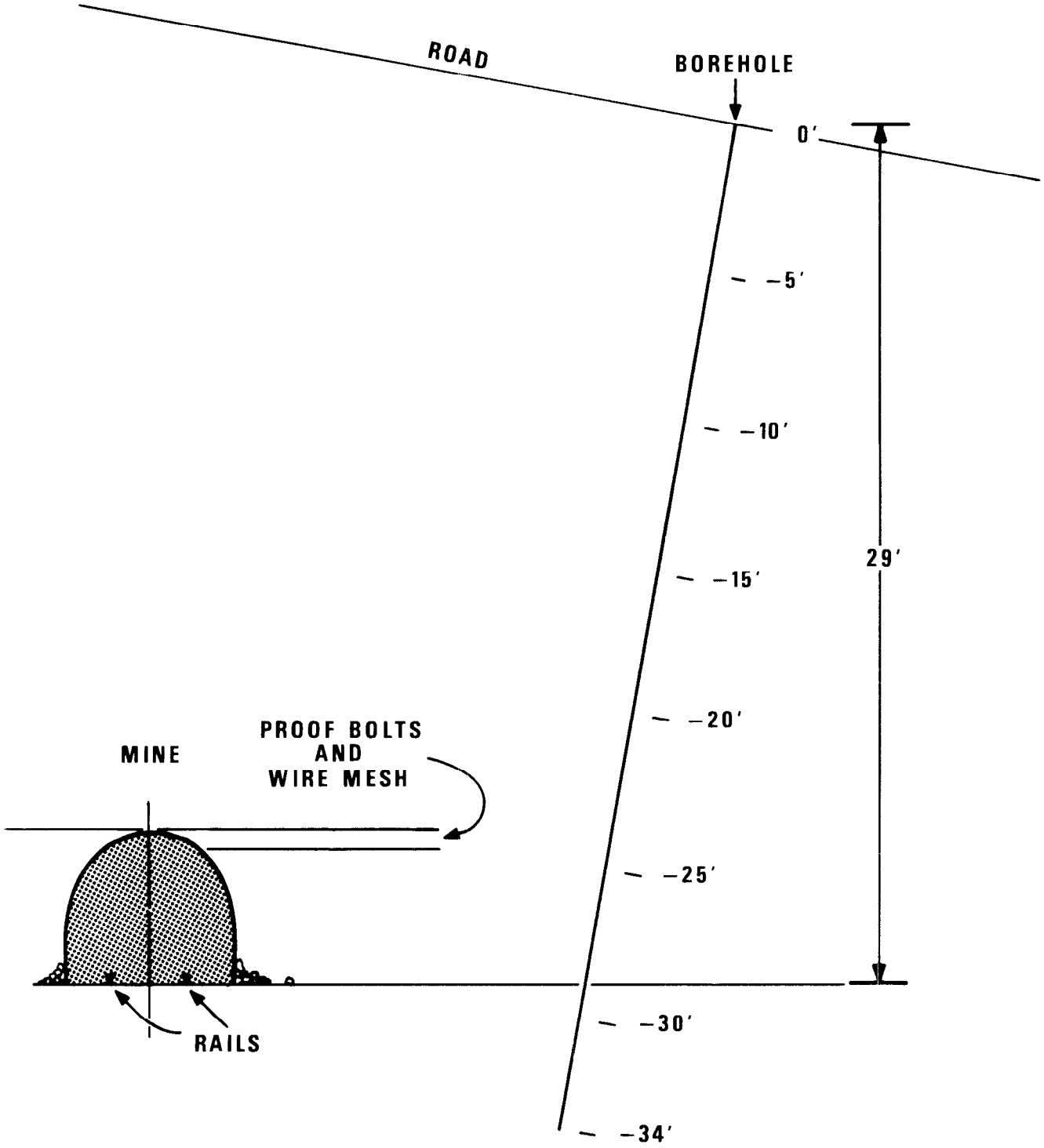

Figure 24. Cross sectional view of borehole and CSM Experimental mine.

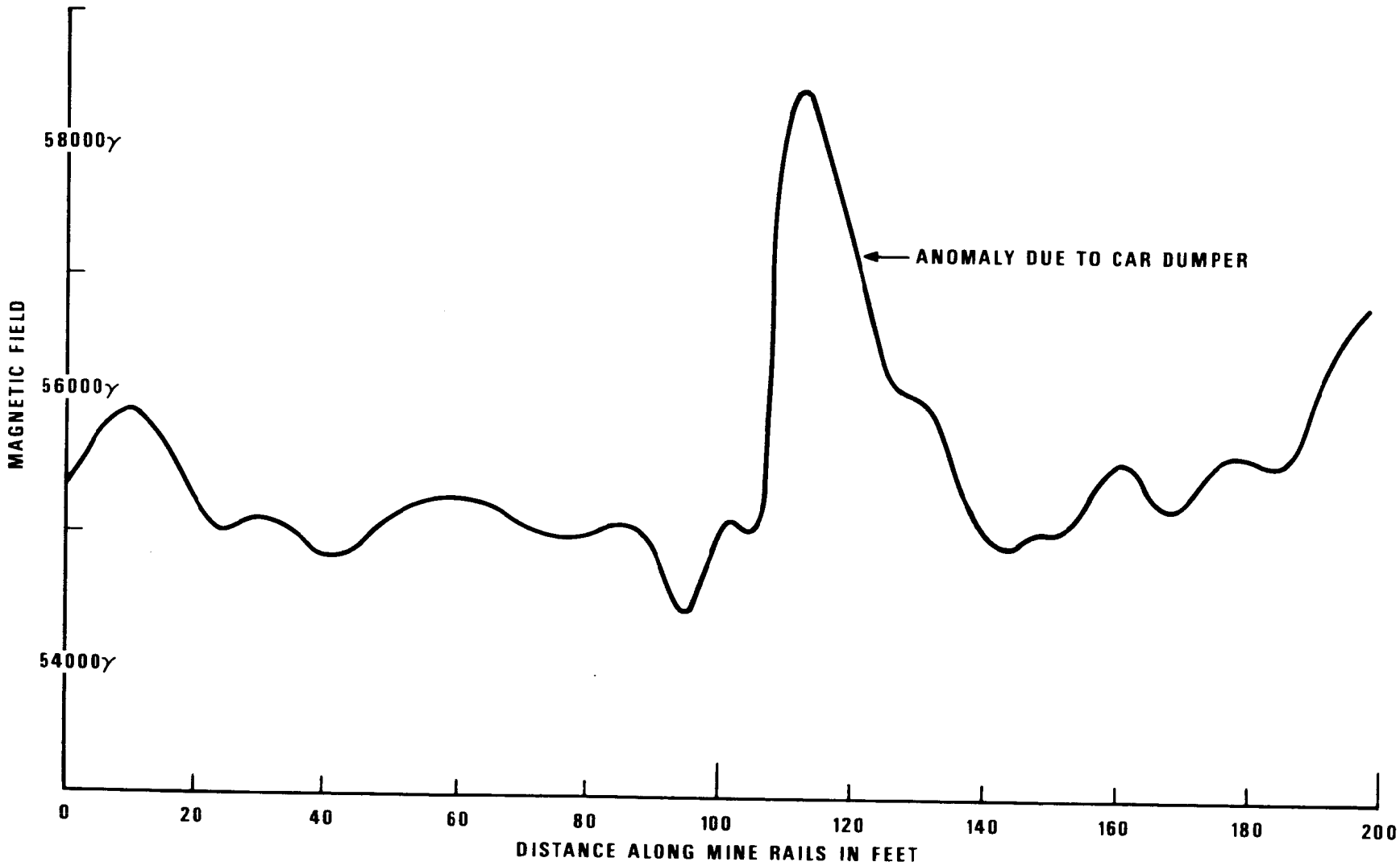

Figure 25. Magnetic survey over mine rails at CSM Experimental mine.

The main anomaly (3000 gammas) is due to a mine car dumper, a 2 foot high by 6 foot long iron hump along the inside rail designed to dump the cars over the edge of the slag pile.

The borehole survey is shown in Figure 26. Repeated surveys all show the same results. The main anomaly is not due to the rails. Rather it occurs at the mine roof level and is due to the proximity of roof bolts, wire mesh, and steel reinforcements. The readings at this level are always erratic which is indicative of iron wire loops. The probable mechanism is that the impulse field from the magnetometer sensor magnetizes these iron loops and the loop residual magnetism varies from reading to reading.

Conclusions on the Magnetic Experiment

As a result of our experiments with the proton magnetometers we arrive at the following conclusions:

1. The rail magnetic anomalies are the size expected but they oscillate.
2. The oscillation half-wavelength seems to correlate with the length of the rail sections.
3. These oscillations further obscure already weak anomalies from the rails in surveys over the railroad tunnels.
4. We tried computing gradients of the magnetic field in an effort to enhance an anomaly of one sign parallel to the rails. However the gradient does not help to detect the rails appreciably.
5. Moving trains cause erratic readings of 1000 gammas or more and are easy to detect on magnetometers even when they are placed 150 feet above the rails.
6. Vehicles (buses, trucks) moved into or out of the vicinity of the magnetometers, 100 feet or more away, give similar (20 gammas to 100 gammas or more) changes to the background field. Such changes in the background (vehicle removed from vicinity within 10 to 30 seconds) are easy to detect.
7. Nearby wires and loops of magnetic material show up easily (a few 100 to 1000 gammas or more) often by erratic behavior or repeated readings.
8. Borehole surveys show promise, but surface magnetometer surveys do not, especially when the sensor to rail depth of burial is greater than 20 to 30 feet.

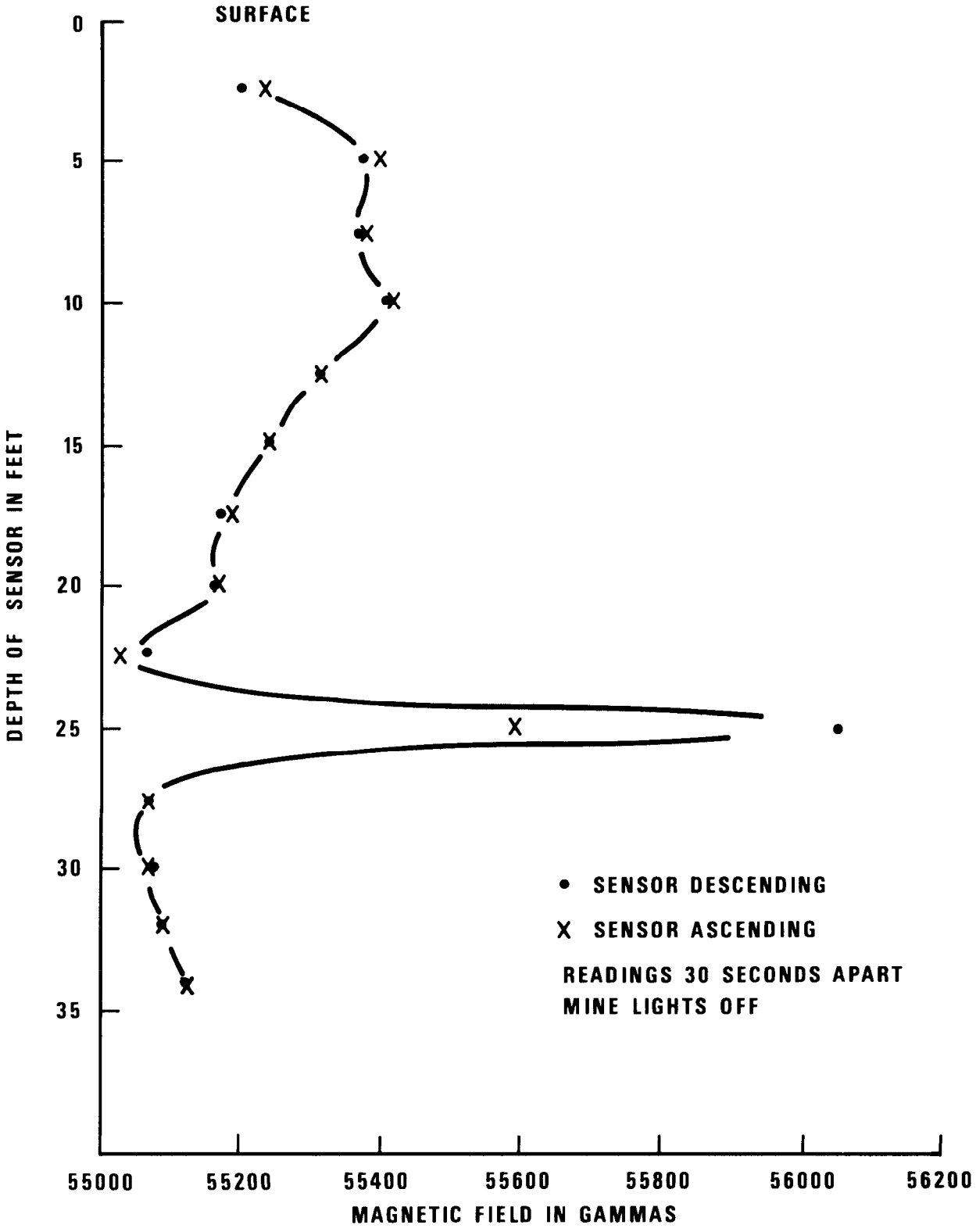

Figure 26. Borehole magnetometer survey at CSM Experimental mine.

ACTIVE SEISMIC METHODS

An active seismic experiment is one which uses dynamite or some other source of compressional waves with a geophone and recording system listening to the response of the medium. Such a system is in contrast to a passive seismic system which detects and locates whatever is going on, be it earthquakes, quarry blasting, or tunneling activity. This study is concerned only with the detection of tunnels by an active seismic system. The objective is to test whether seismic exploration techniques can detect an underground tunnel by reflection or refraction evidence.

Cook (1965) shows that underground cavities can be detected by seismic reflections when the cavity dimensions (diameter of the tunnel) are the same order of magnitude or larger than the wavelength of the reflected seismic energy. Thus for tunnels in granite with P-wave velocities of 16000 feet/second wavelengths of the order of the tunnel diameter (25 feet) would require appreciable seismic energy at 640 Hz.

$$f = \frac{v}{\lambda} = \frac{16000 \text{ ft/sec}}{25 \text{ ft/sec}} = 640 \text{ Hz.}$$

Watkins, et al. (1967) demonstrated another method of seismic detection of near-surface cavities. This method, which detects oscillations of the cavity walls on the geophones directly over the cavity, is based upon a theoretical development by Biot (1952). According to Biot's group velocity curves, we have for a cylindrical hole in an infinite solid:

$$f \cong \frac{V_s}{1.55D}$$

where V_s is the shear-wave velocity, D is the diameter of the cylinder, and f the resonant frequency of the cavity wall oscillations. Our field experiments were designed to test both methods for detecting tunnels.

We used a standard exploration seismic system owned by the Colorado School of Mines and built by SIE. Figure 27 shows a photograph of the instrument recording truck and the geophone implacements along the road. We used

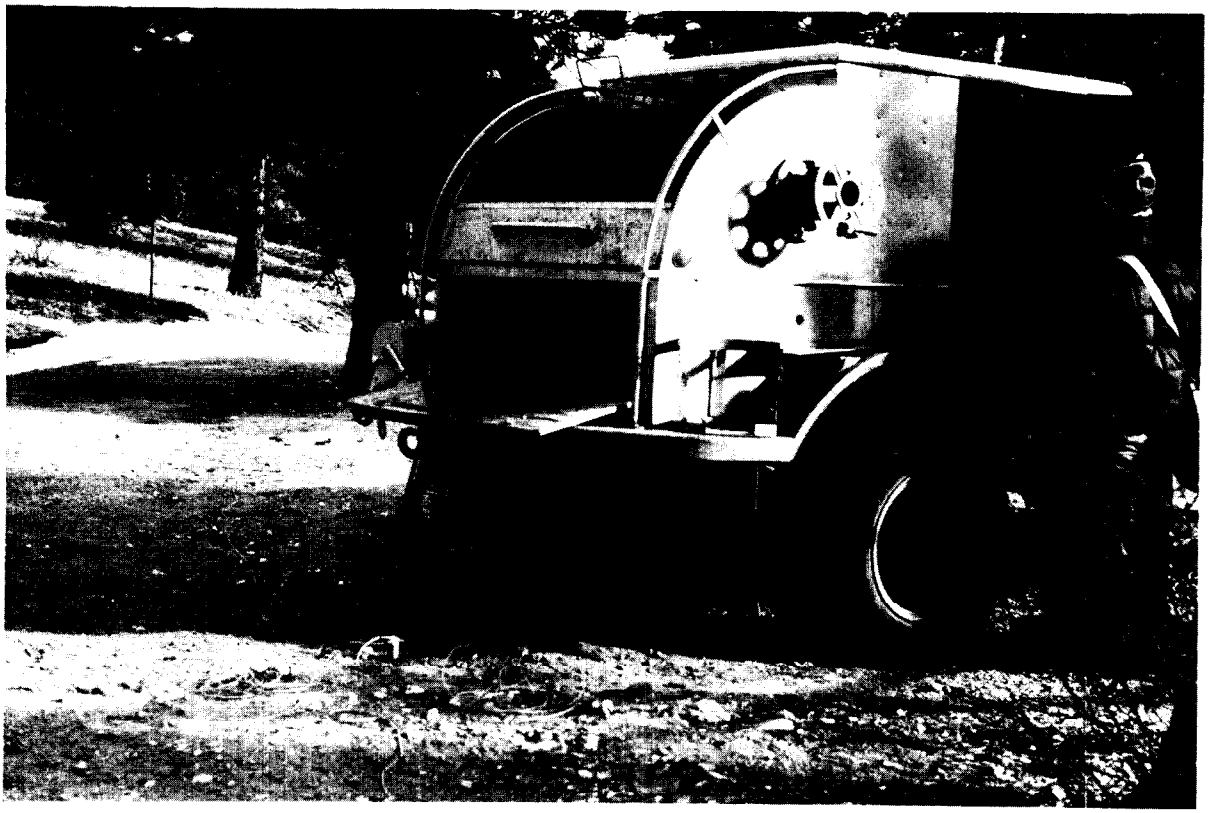

Figure 27. Seismic recording truck of Colorado School of Mines.

both 6 geophones per channel and a single geophone per channel, 24 channels, digital and analog tape recording, geophones of the Hall-Sears Junior style. (See Appendix A for their characteristics.)

Sources used included dynamite caps and the Dinoseis, a truck-mounted cylinder filled with propane and oxygen and exploded while in contact with the ground. Figure 28 shows a photograph of the Dinoseis truck.

Other equipment and sources included the Bison hammer seismograph, (Bison Manufacturing Company, Minneapolis, Minnesota). A sledge hammer blow on the ground is recorded by a single geophone onto an oscilloscope with a digital memory. Subsequent blows can be added (stacked) to the original permitting shot-array procedures. In addition to the oscilloscope a paper recorder can provide a permanent record of any desired seismogram showing on the oscilloscope. Figure 29 shows a photograph of the Bison oscilloscope and recording units.

The primary sites chosen were two tunnels of the DRGW Railroad near Eldorado Springs, Colorado. They are single track, in granite, and possess fairly easy equipment access over the tunnel. The road is 250 feet above the Tunnel-17 and 120 feet above Tunnel 19. Figure 30 shows the seismic profile over Tunnel 19; the setup over Tunnel 17 is similar. Railroad tunnels are larger than the mines we are seeking. However, we expected considerable difficulty in seeing the tunnels seismically because the seismic wavelengths are so long compared to the cross section dimensions of any tunnel. If the seismic method will not work on a railroad tunnel, we would not expect it to work on a mine. Other advantages of the railroad tunnels are that they exist singly and are well mapped. In contrast most of the mines in Colorado exist in multiple shafts and drifts and are poorly mapped making a controlled experiment difficult.

There are four Dinoseis records taken at each of the 24 geophone stations plus six more beyond each end of the geophone spread. The four common shot-point records were added. Figure 31 shows a few of these seismograms where the Dinoseis souce is near the center of the spread. The complete set of these plots are reproduced by the Phoenix computer of the Seismograph Service Corporation in Denver.

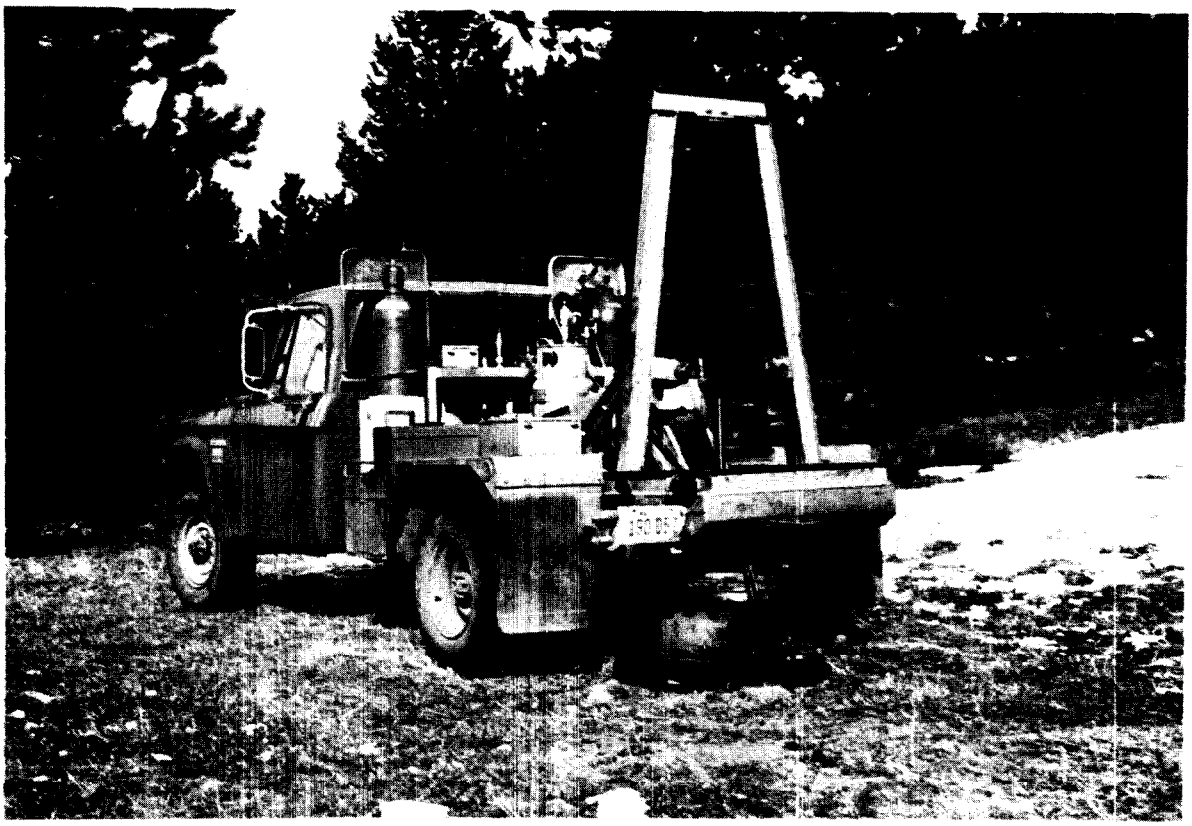

Figure 28. Dinoseis truck.

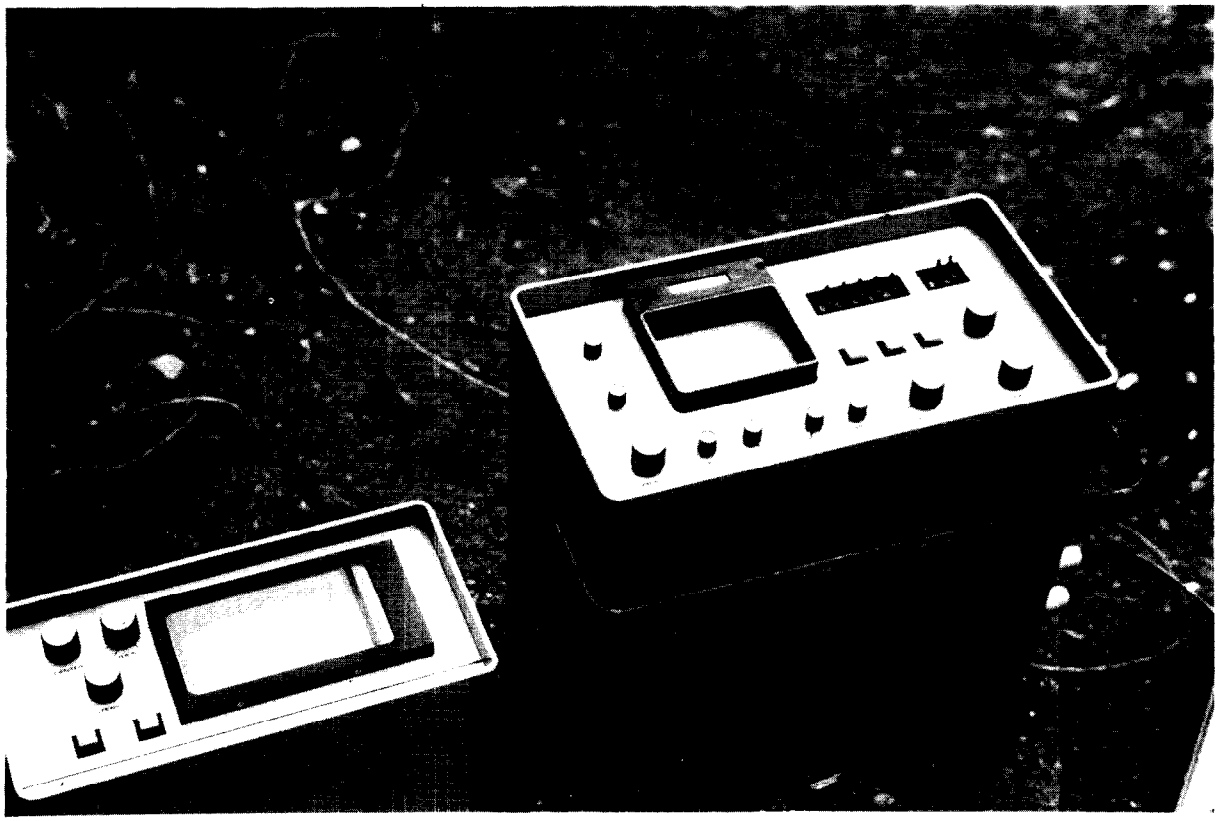

Figure 29. Recording units of the Bison hammer seismograph.

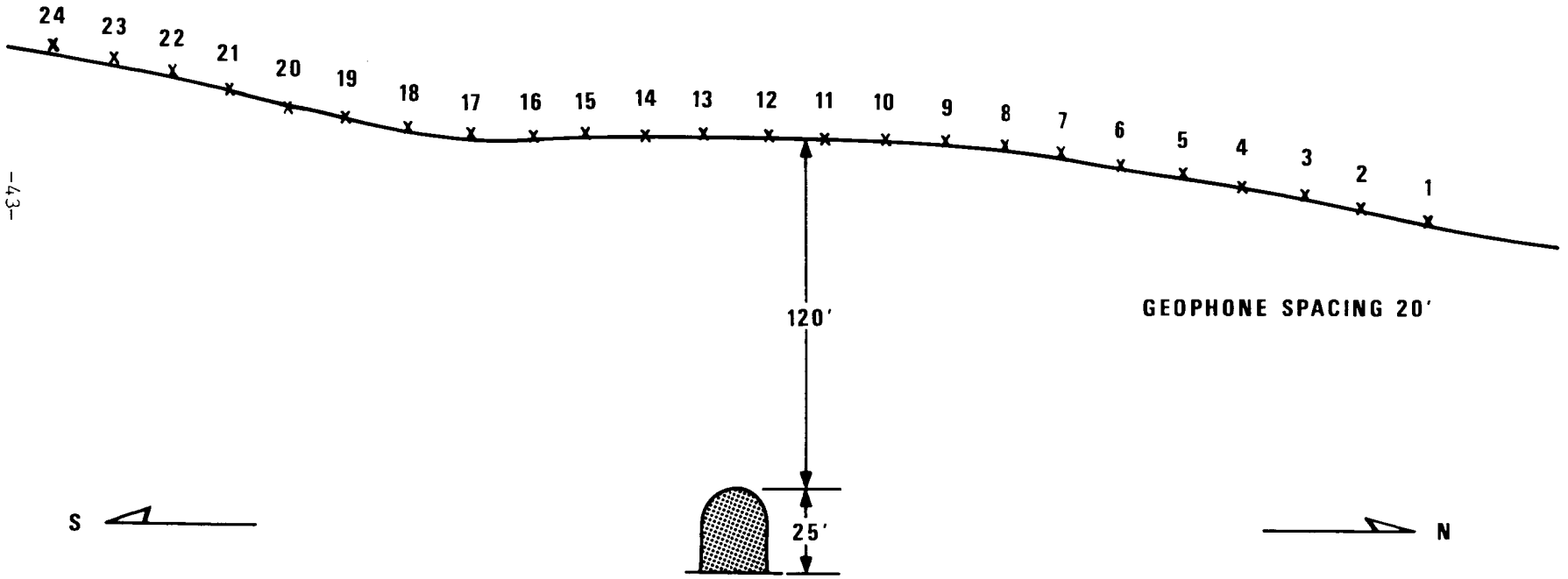

Figure 30. Seismic profile over Tunnel 19, DRGW Railroad.

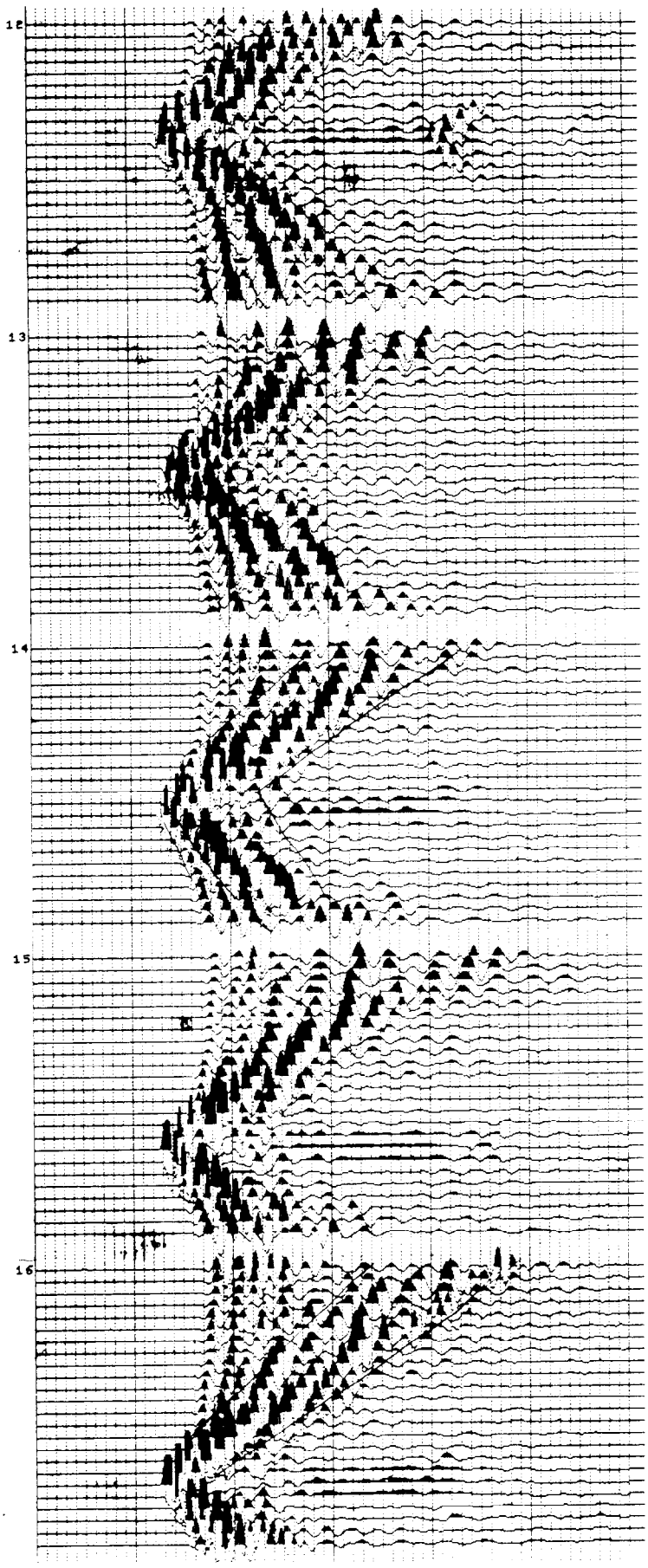

Figure 31. Center set of Dinoseis records taken over Tunnel 19, DRGW Railroad.

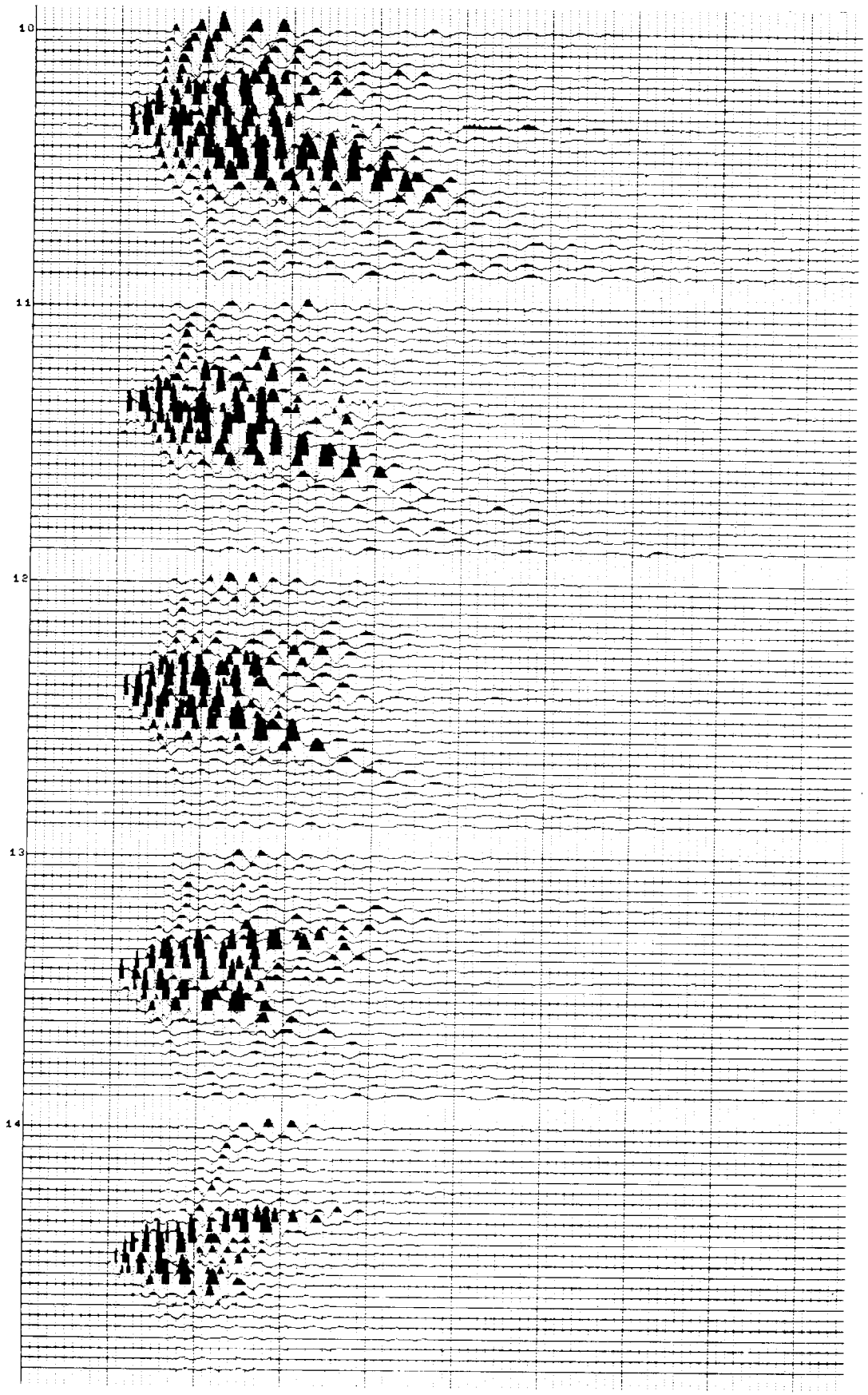

Figure 31 continued. Center set of Dinoseis records taken over Tunnel 19, DRGW Railroad.

The Dinoseis uses two time breaks, one from the recording truck triggering a second from the Dinoseis truch which actually fires the shot. The programs in the Phoenix computer respond to the first time break whereas the first arrivals are consistant with the second one. Since there can be 10 to 20 milliseconds variation between the two, static time corrections had to be entered into the Phoenix computer to align the four common shot point records. As a result of this adjustment the Phoenix computer has aligned the second time break at the 0.1 second mark which becomes the time origin for these plots.

In addition a time correction for weathering and the one-way travel time to the top of the tunnel was applied to each of the 23 different shot-point records along the spread. Then these 23 records with both static and dynamic corrections were summed together yielding the single record playout shown on Figure 32.

The objective of summing the 23 corrected records was to suppress coherent noise and enhance any diffraction patterns emanating from the tunnel. If the diffraction effect from the tunnel is present, it is not readily apparent.

Similar computations were applied to the data from the Tunnel 17 profile. Figure 33 shows the center records with no corrections applied. The remaining seismograms are shown in the Appendix. Again no reflection evidence of the tunnel is apparent.

Two kinds of stacking procedures were applied to the Tunnel 17 data. The first shown on Figure 34 is conventional where corrections for two-way travel time are applied. The second on Figure 35 shows three records with the static and dynamic corrections applied as for Tunnel 19. The center record has been corrected to a one-way travel time where the tunnel is. The other two records have been corrected to the top of a tunnel under one or the other end of the profile where, of course, there is no tunnel. If this stacking operation were helping, the center seismogram would look appreciably different than the other two. It does not.

A major problem arises from the presence of a low velocity layer. Figure 36 shows the geophone spread and two layer cross section over Tunnel 17.

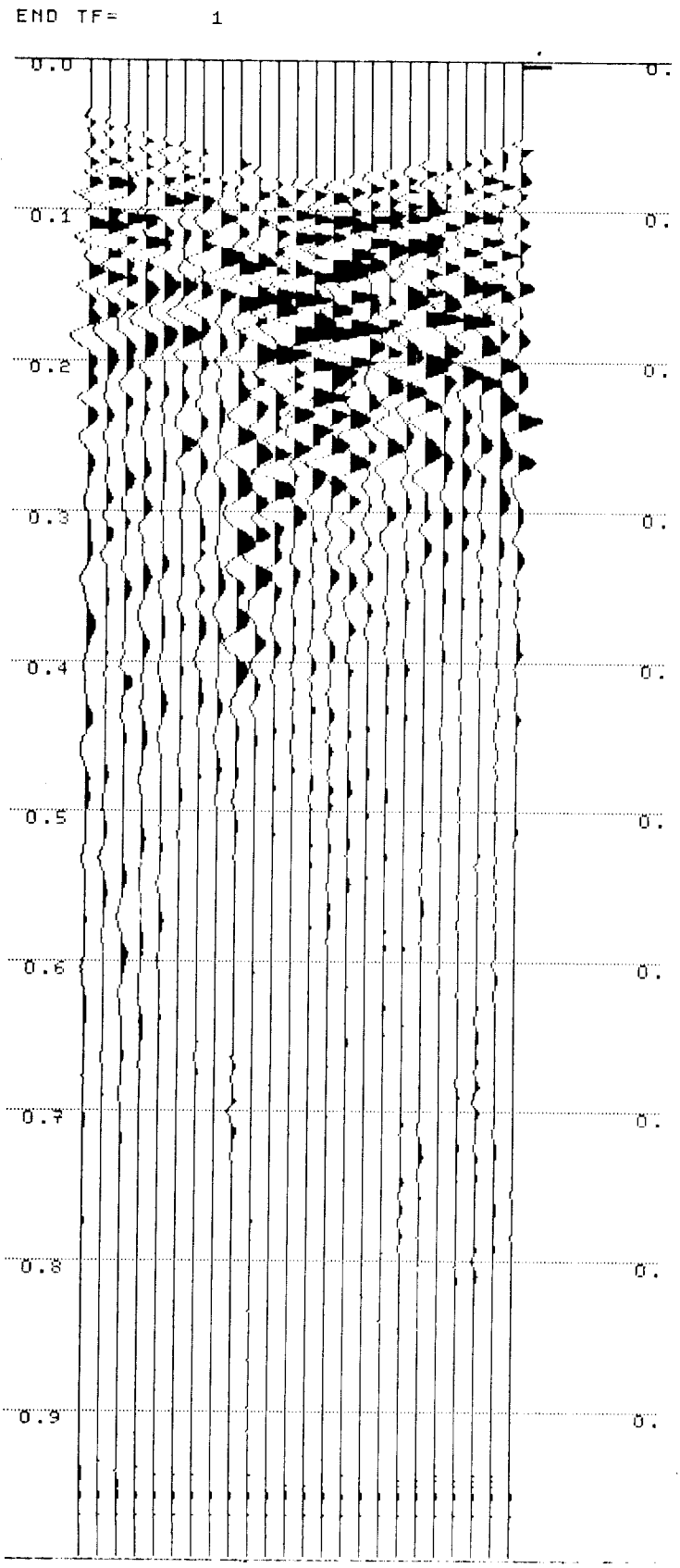

Figure 32. Summation record over Tunnel 19 with static and dynamic corrections applied.

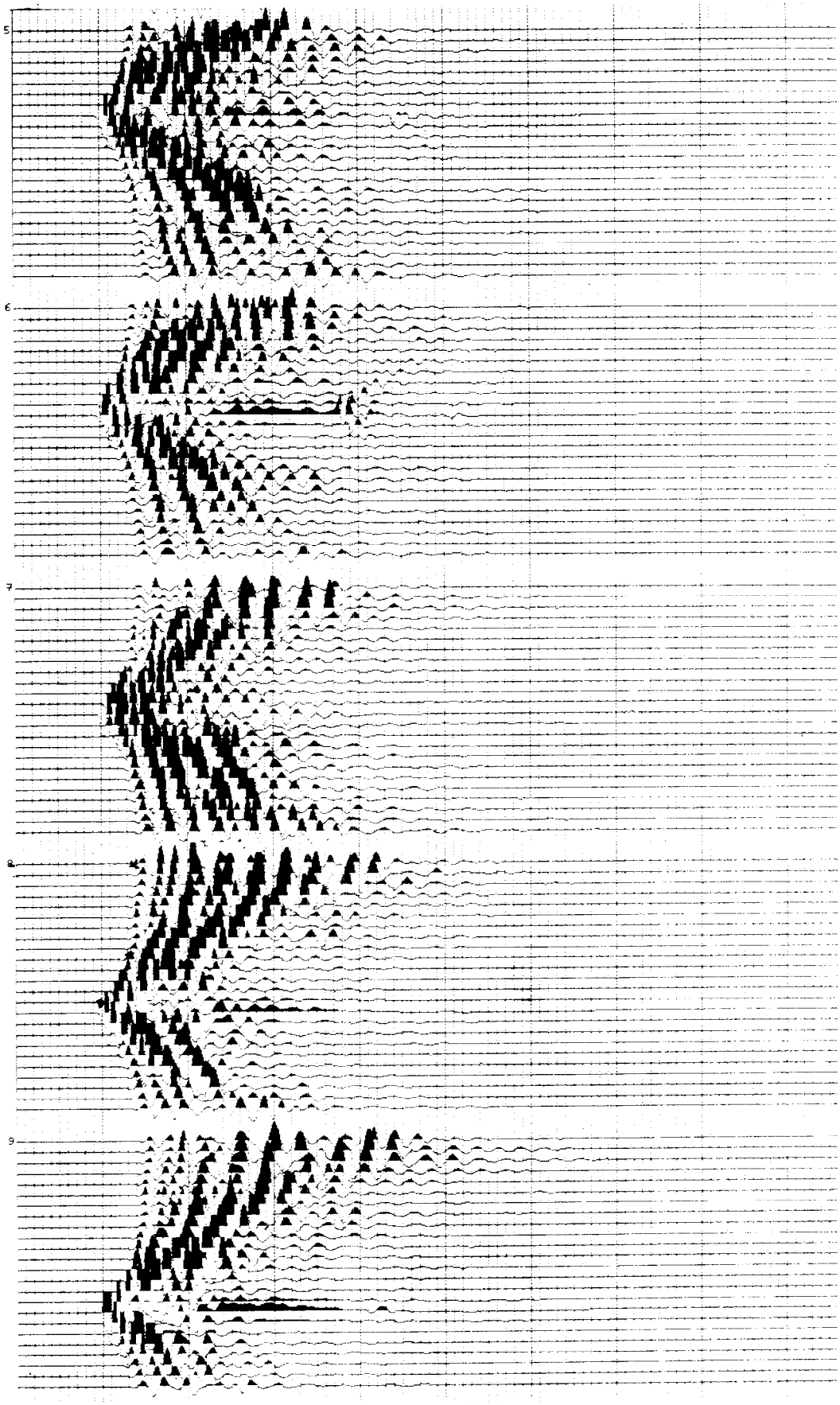

Figure 33. Center set of Dinoseis records taken over Tunnel 19, DRGW Railroad.

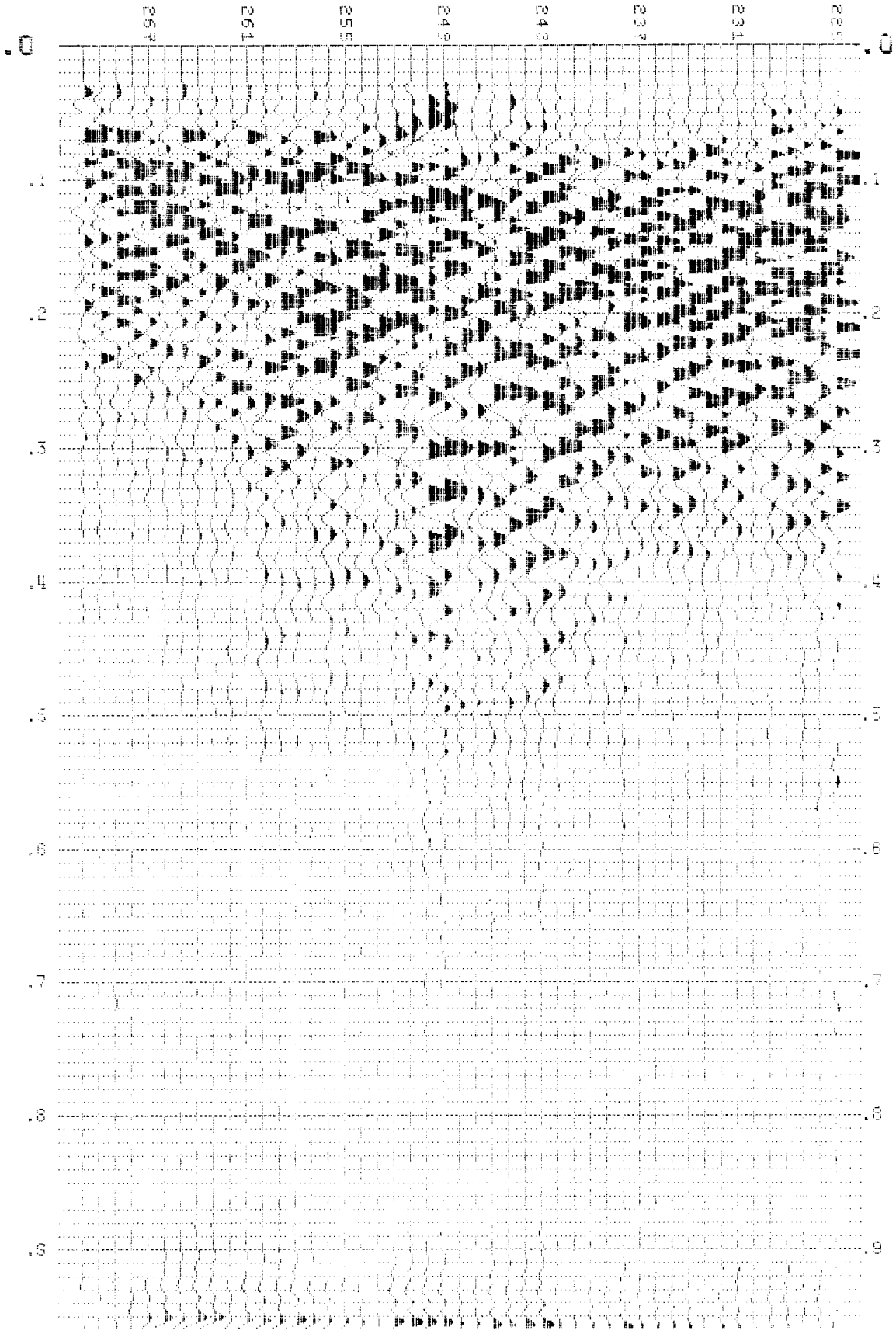

Figure 34. Conventional stacking of Tunnel 17 data corrected for two-way travel times to tunnel. -49-

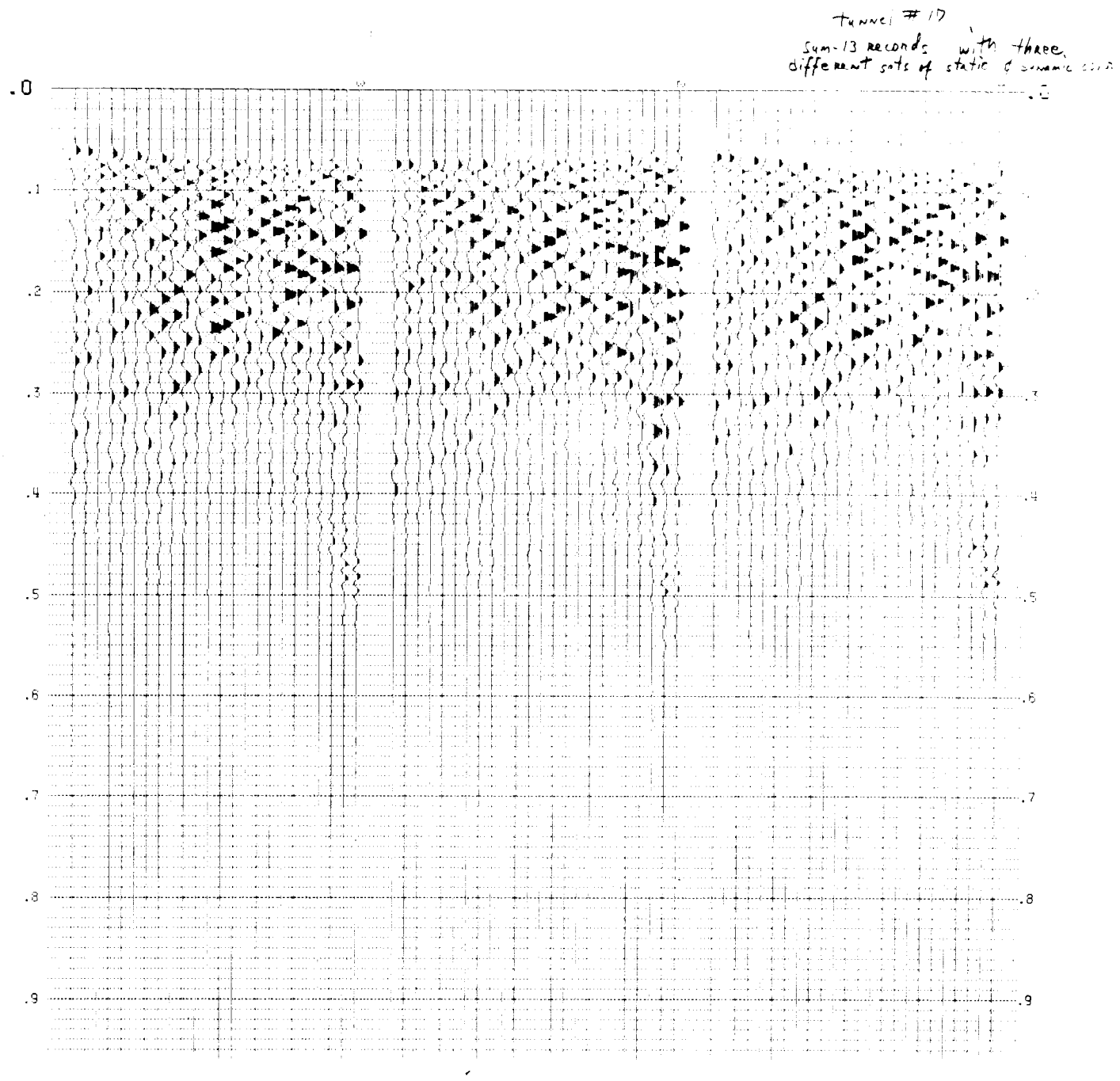

Figure 35. Three stacked records over Tunnel 17, assuming a tunnel at the south end, center, and north end respectively.

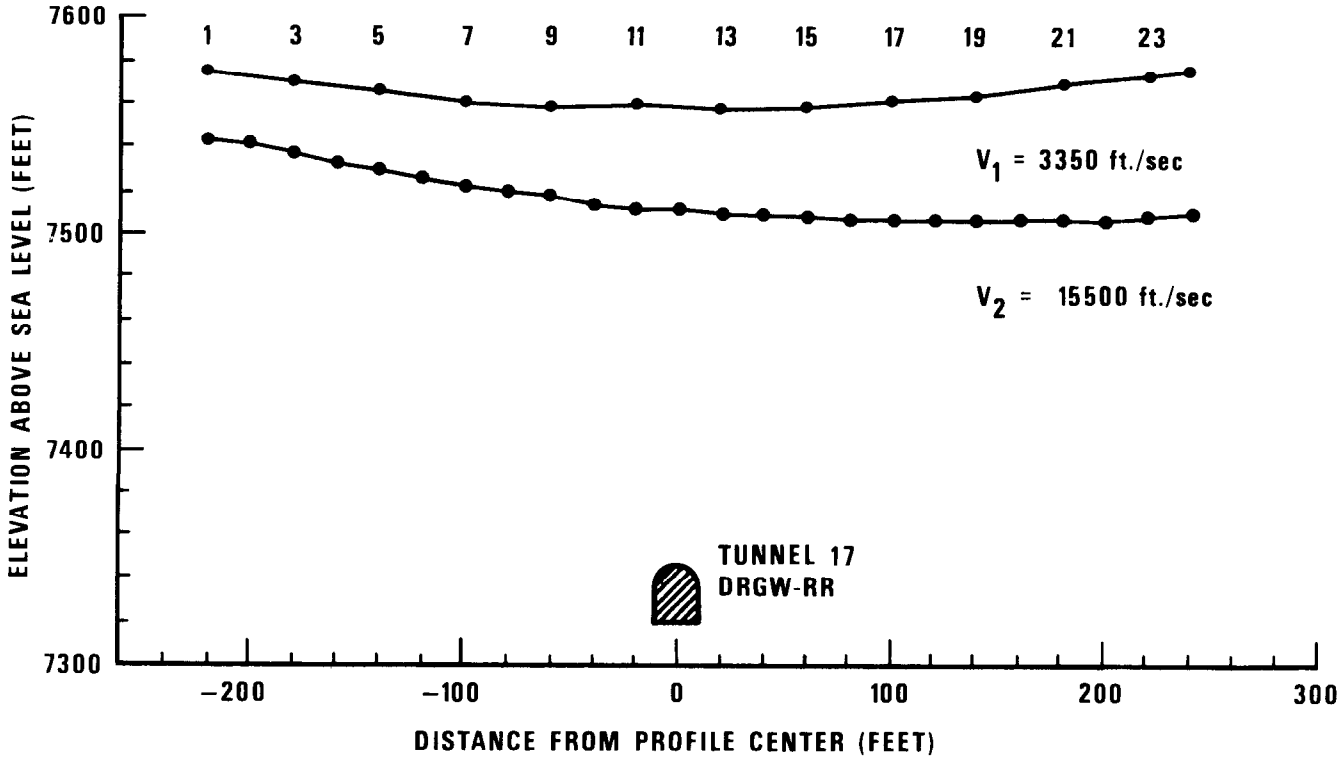

Figure 36. Seismic cross section over Tunnel 17, DRGW Railroad.

An analysis of first breaks shows that the upper layer has a velocity of 3350 feet/second whereas the lower medium with the tunnel has a velocity of 15,500 feet/second. Since the sine of the critical angle is V_1/V_2, all energy more than 12.5° from the vertical will be totally reflected. Thus less than 14% (ratio of 12.5°/90°) of the energy from the source will penetrate the lower layer. The seismograms are showing mainly the energy trapped in the upper layer.

Other negative evidence comes from Biot's (1952) relation for the resonance of the cavity walls. With a shear velocity of 3800 meters/second in granite and a tunnel diameter of 8 meters, the expected resonnant frequency, f, of the tunnel walls would be:

$$f = \frac{V_s}{1.55D} = \frac{3800 \text{ m/sec}}{12.4 \text{ m}} = 307 \text{ Hz}$$

which is significantly higher than the 50 Hz energy on the records.

Better evidence of tunnel reverberations showed up with the Bison equipment over a coal mine. A coal seam at Walden, Colorado was being strip mined by the Kerr Coal Company when one piece of equipment fell into an old coal mine which was not known to be there. Bison records show the differences over solid coal and over cavities (see Figure 37). The response over solid coal is impulsive; the response over the stope reverberates for several cycles longer.

We contoured the map in two levels, cross hatching the area where reverberation records were recorded and leaving blank the area where impulsive records were recorded (see Figure 38). We postulate that the reverberations lie over the route followed by the old coal mine. As of this writing the coal strip mining has not proceeded far enough to verify the precise route of the mine.

Conclusions on the Seismic Experiments

As a result of our seismic experiments we concluded:

1. No reflection evidence of the railroad tunnels showed up on our records, whether the sources were Dinoseis, dynamite caps, or Bison hammer.

2. The stacking of two dozen seismograms to enhance diffraction patterns from the top of the tunnel was not successful.

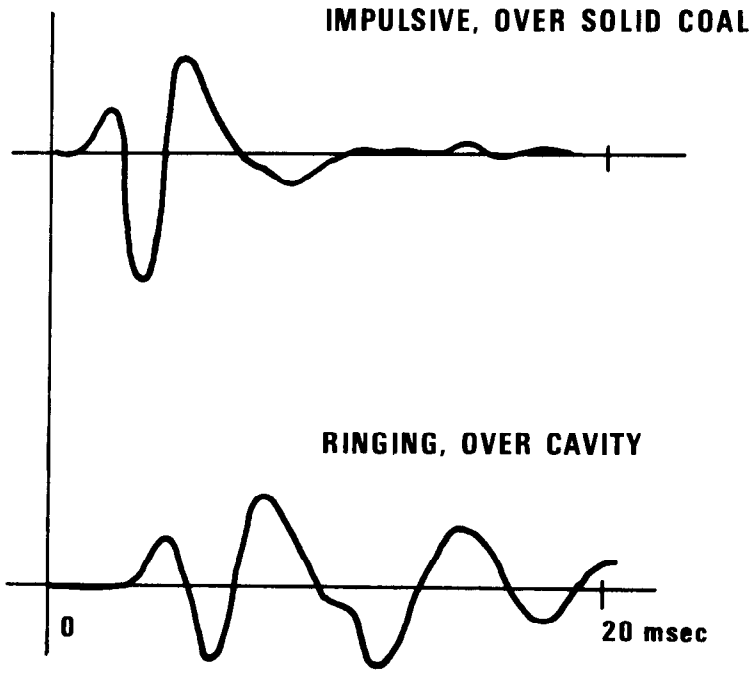

Figure 37. Typical Bison records over coal mine.

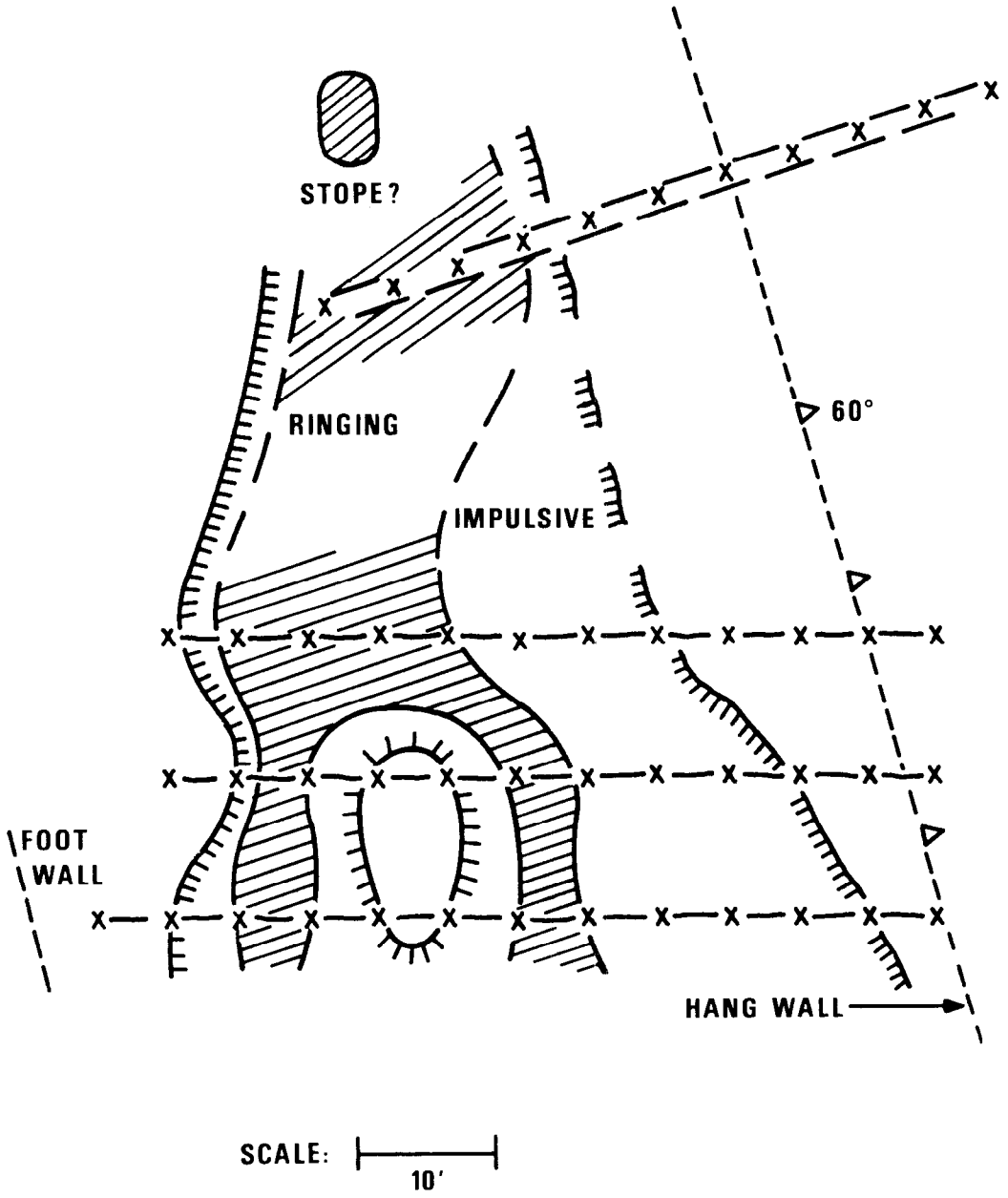

Figure 38. Map over coal seam with contours showing region of reverberation seismograms.

3. No evidence of wall reverberations as reported by Watkins (1967) appeared on the seismograms over the railroad tunnels.

4. The primary problem was a low velocity layer over the granite which trapped most of the seismic energy. Hence very little energy penetrated the granite layer which contained the tunnel.

5. Some evidence of tunnel wall reverberations appeared over a coal mine. At this site although the tunnel is smaller, there was no low velocity layer (coal outcropped and was being strip mined) and the P-wave velocity is much lower than that for granite.

6. Seismic field experiments to detect tunnels by reverberations of the walls should be conducted using multichannel (24) seismic systems rather than single channel systems like the Bison. Neighboring traces from single channel systems are often difficult to correlate.

ESTIMATION OF THE DETECTABILITY OF MINING ACTIVITIES BY MONITORING AIRBORNE Rn^{222}

The detection of a source of radioactive gas for given conditions of atmospheric stabiilty depends primarily on the source strength (Q), the wind velocity ($\bar{u}$), and the limit of detection (χ).

For a mining operation which advances 4 meters per day with a cross section of 4 m^2, Q is calculated as follows for granite based on the parameters in Table 1. Metamorphic rock is assumed to be the same composition as granite and basalt is omitted because it averages five times less uranium than granite.

TABLE 1

Volume of rock mined,	$V = 16\ m^3$/day or 16×10^6 cc
Uranium content for granite,	$U_g = 25 \times 10^{-6}$ g U/g rock (upper range)
	4×10^{-6} g U/g rock (average)
The specific activity of U,	$U_s = 0.332\ \mu Ci/g\ U^{238}$
	$\mu Ci = 2.2 \times 10^6$ disintegrations per minute (dpm)
The density of granite,	$\rho = 2.8$.

Since Rn^{222} is a daughter of U^{238} only and the highest concentration that can exist in the activity in equilibrium with the parent isotope, the Rn^{222} activity in a rock will be equal to the U^{238} activity of 0.332 μCi/g U. Since $U_g = 25 \times 10^{-6}$ g U/g rock the total Rn^{222} activity = 8.3×10^{-6} μCi/g rock if the upper range of U in granite is chosen. The amount of rock mined per day is $V\rho = 16 \times 10^6$ cc x 2.8 g/cc = 45×10^6 g. The source strength, Q, is 8.3×10^{-6} μCi/g rock x 45×10^6 g rock/day or 375 μCi/day if we assume that <u>all</u> of the available Rn^{222} escapes from the rock material.

Although the detection limit of Rn^{222} is very low in the laboratory, the practical limit of detectability in the natural environment is limited by the natural background which is omnipresent and quite variable depending mainly on wind velocity, atmospheric stability, barometric pressure, and uranium

content of the terrain. A concentration of $\chi = 10^{-6}$ $\mu Ci/m^3$ (2.2 dpm/m^3) would probably not be detectable above background, but let us for purposes of illustration take this level as the minimum detectable level (MDL). The ground level (2 m) concentration of α-active aerosols (regarded as representative of Rn^{222} concentration) was found by Kirichenko (1970) to vary from 2×10^{-4} to 6×10^{-4} $\mu Ci/m^3$ and a typical value given by Rankama and Sahama (1949) is 10^{-4} $\mu Ci/m^3$, so the value of $\chi = 10^{-6}$ $\mu Ci/m^3$ for background is probably too low by a factor of 100 even if a signal to noise ratio of 1:1 could be accepted.

The areas over which a given source of radioactive gas is detectable have been calculated for a variety of combinations of atmospheric stability, wind velocity, detection limit, and source strength. The relation between detection limit, source strength and wind velocity reduces to a single parameter $(\chi/Q)\ \bar{u}$ which has the units of $\mu Ci/m^2$. For $\chi = 10^{-6}$ $\mu Ci/m^3$, Q = 375 $\mu Ci/d$ and a wind velocity of 1 mph (.44 m/sec):

$$\frac{\chi}{Q}\ \bar{u} = \frac{10^{-6}\ \mu Ci/m^3}{375\ \mu Ci/d}\ (.44\ m/sec)\ (86{,}400\ sec/day)$$

$$= 1.0 \times 10^{-4}\ \mu Ci/m^2.$$

The larger this quantity, the smaller will be the area of detection. Therefore, an increase in wind velocity or detection limit, or a decrease in source strength will decrease detectability.

The area of detectability calculated for moderately stable conditions and $(\chi/Q)\bar{u} = 1 \times 10^{-4}\ m^{-2}$ gives a maximum range of detection of 1 km for a stationary sampler directly downwind from the source.

Since we have taken the most optimistic parameters, i.e., moderately stable atmospheric conditions, wind velocity of 1 mph, a signal to noise ratio of less than 1, total release of all Rn^{222} in the rock, and a granite with the upper range of uranium content, we can conclude that it is highly unlikely that mining activities of the type contemplated can be detected at useful distances by monitoring airborne Rn^{222}.

If the calculations were carried out using what might be termed a "reasonable" set of parameters rather than the "conservative" values used we would have

U_g = 4 μg/g so Q = 60 μCi/d

χ = 10^{-4} μCi rather than 10^{-6} μCi/m^3

and $\overline{u}$ = 5 mph rather than 1 mph.

$(\chi/Q)\overline{u}$ would be a factor of 3000 larger and the area of detectability would actually be extremely small.

REFERENCES

Biot, M. A., 1952, "Propagation of elastic waves in a cylindrical bore containing a fluid", Jour. Appl. Physics, Vol. 23, pp. 997-1005.

Breiner, S., 1973, "Applications manual for portable magnetometers" printed by Geometrics, Inc., 914 Industrial Ave., Palo Alto Calif. 94303, USA.

Cook, John C., Aug. 1965, "Seismic mapping of underground cavities using reflection amplitudes"; Geophysics, Vol. 30, No. 4, pp. 527-538.

Godson, R. H. and Watkins, J. S., "Seismic resonance investigation of a near-surface cavity in Anchor Reservoir, Wyoming", Bull. Assoc. of Engr'g. Geologists, Vol. V, No. 1, pp. 27-36.

Kirichenko, L. V., 1970, "Radon Exhalation from Vast Areas according to Vertical Distribution of its short-lived decay products", Jour. Geophys. Res., Vol. 75, No. 18, pp. 3639-3649.

Rankama, K. and Sahama, T. G., Geochemistry, the University of Chicago Press, Chicago, 1949.

Watkins, J. S., Godson, R. H., and Watson, K., 1967, "Seismic detection of near-surface cavities", Professional Paper 559-A, U. S. Geological Survey, pp. 1-12.

ACKNOWLEDGEMENT

The author gratefully acknowledges the help received in conducting this study and writing the report. Dr. Donald Schutz of Teledyne Isotopes conducted the study and wrote the section on Radon decay. Dr. Phillip Romig of the Colorado School of Mines (CSM) directed the seismic field efforts and acted as chief consultant throughout the project on the seismic and magnetic methods. Mr. Jim Callaway of CSM did the weathering and derived the seismic cross section as well as conducted the data processing at SSC's Phoenix Computer. Mr. Steven Peterson of CSM measured the frequency responses of the Hall-Sears geophones.

APPENDIX A

APPENDIX A

Response Curves for Geophones (Hall-Sears-Junior type) on the Shaking Table

Apparatus

1. Audio oscillator and power amplifier (GRC 1308-A)
2. Oscilloscope (Tektronix 561, with plug-in units 63 and 67)
3. Colorado School of Mines shaking table
4. Oscilloscope with transducer and strain gauge preamplifier (Tektronix 531, with plug-in unit G)
5. One string of geophones (Hall-Sears-junior) with 6 geophones per string.

Procedure

The shaking table was operated at a constant displacement for frequencies from 20- to 800-Hz using the apparatus described above and portrayed in Figure 2. The movement of the shake table is monitored by the Tektronix 531 oscilloscope. The voltage output from the geophones is measured by the Tektronix 561 oscilloscope. The peak-to-peak voltage output from the string of geophones was recorded at 20-Hz intervals.

Results

The frequency response of this geophone is shown on Figure A-1. Harmonic distortion is observed for these geophones as follows:

1. From 280- to 340-Hz and from 500- to 600-Hz for a 1/8-micron displacement.
2. From 500- to 600-Hz for a 1/4-micron displacement.
3. From 360- to 400-Hz for a 1/2-micron displacement.

The logarithmic frequency response is nonlinear above 300-Hz.

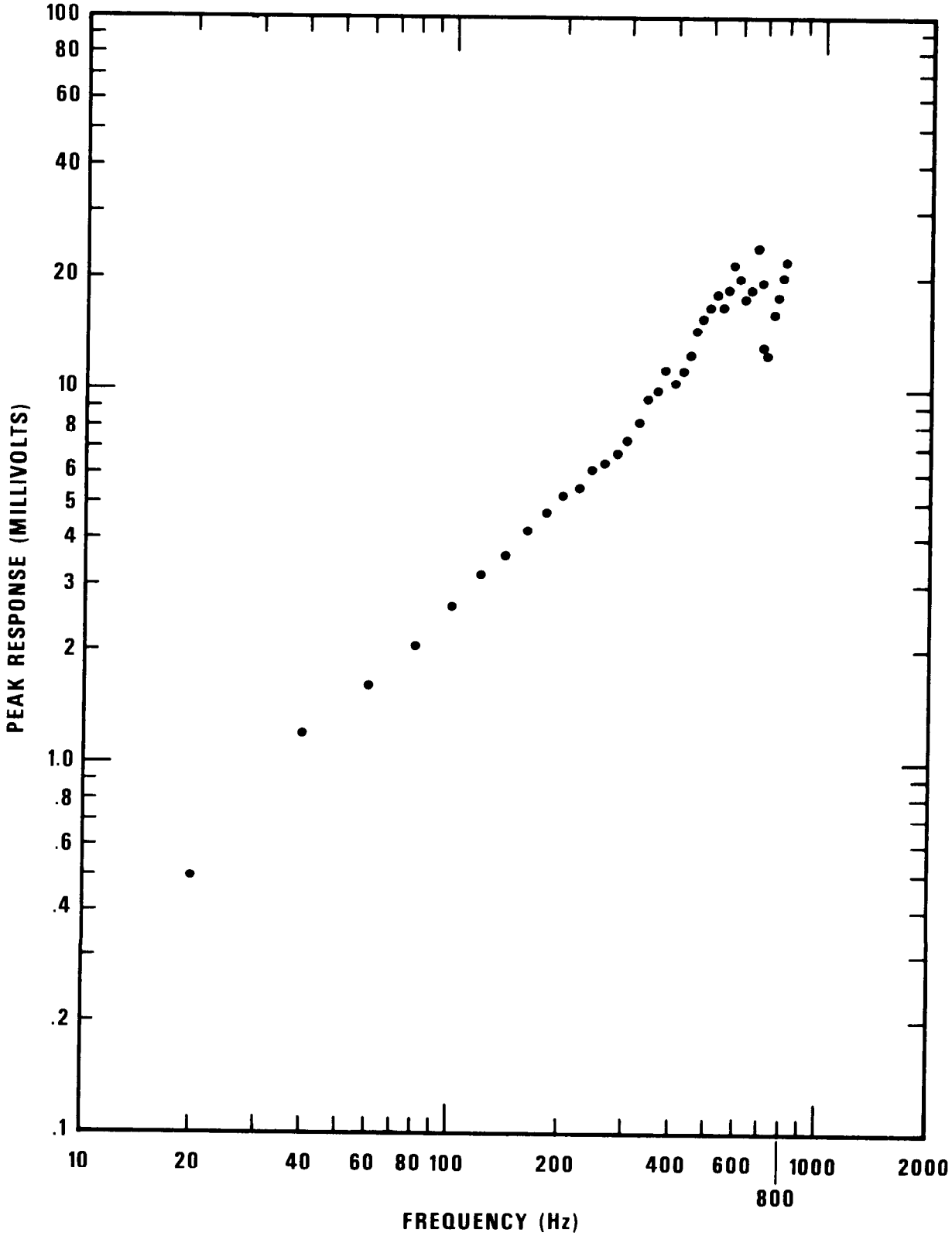

Figure A-1. Frequency response of the Hall-Sears junior geophone.

APPENDIX B

APPENDIX B

Seismograms from north-south profiles over the Denver and Rio Grande Western Railroad Tunnel 19 and Tunnel 17 near Eldorado Springs, Colorado.

Source: 4 Dinoseis shots at each geophone station
Geophones: Hall-Sears-junior
Geophone Spacing: 20 feet
Seismograph: SIE Digital System owned by Colorado School of Mines
Playout: from Phoenix computer of Seismograph Service Corporation, Denver, Colorado.

```
HØRIZØNTAL PLØT RUNNING
AØØ875
SYSØØ875

**** PHØENIX LINE HEADER ***

  JØB ID NØ.          172
  LINE NØ              17
  NØ ØF SAMPLES       500
  SAMPLING RATE         2
  CHANNELS/GRØUP       24
  INPUT CREATED   AØØ875

  INPUT REEL NØ     1905


XC
FØRTRAN IV DN393944 REV.H
START GAIN  (DB)    -27
```

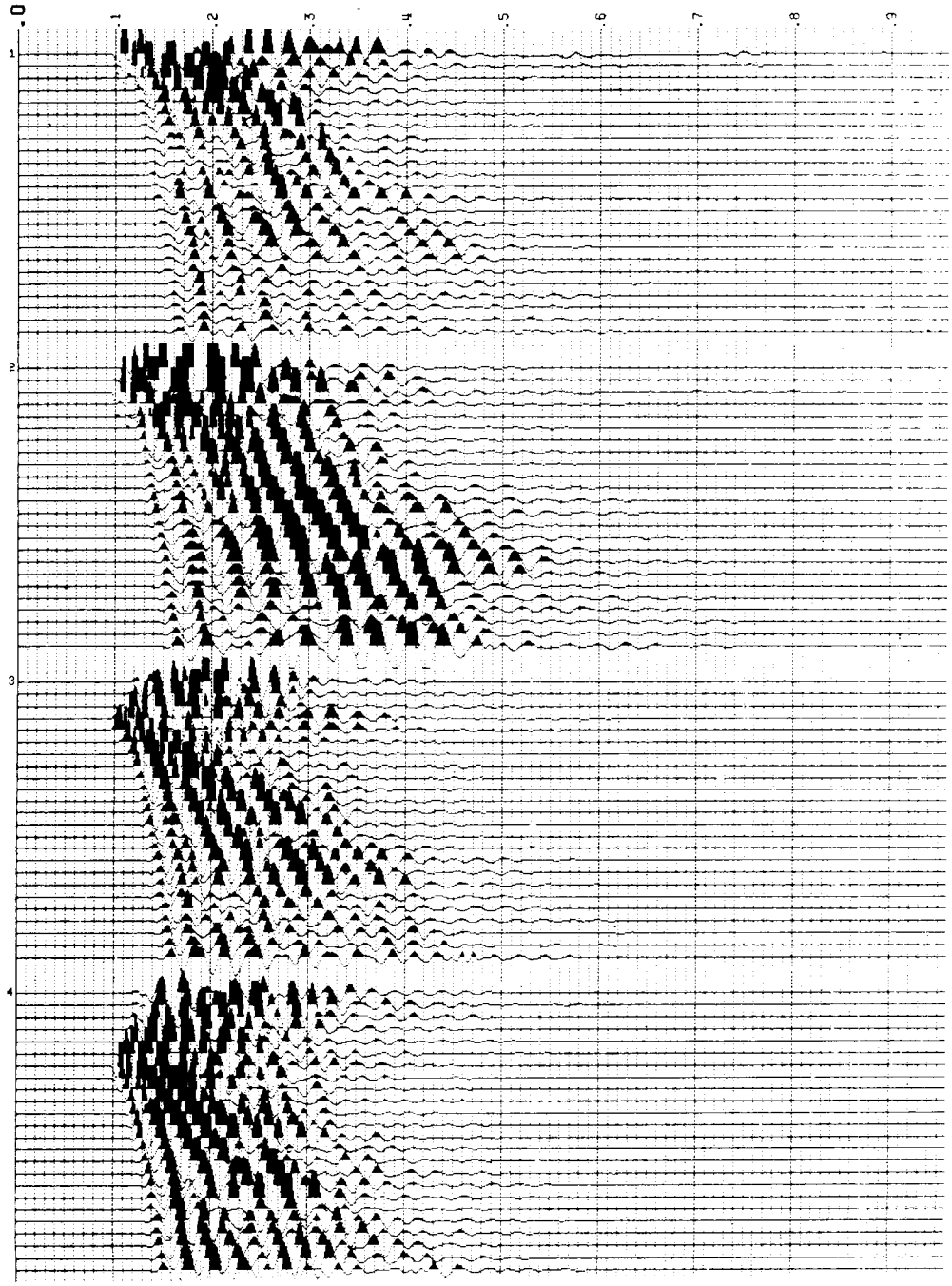

Figure B-1. Tunnel 17, DRGW RR - Sum of 4 Dinoseis records at each shot point. Static corrections added to align 1st breaks. Data time origin at 0.1 seconds.

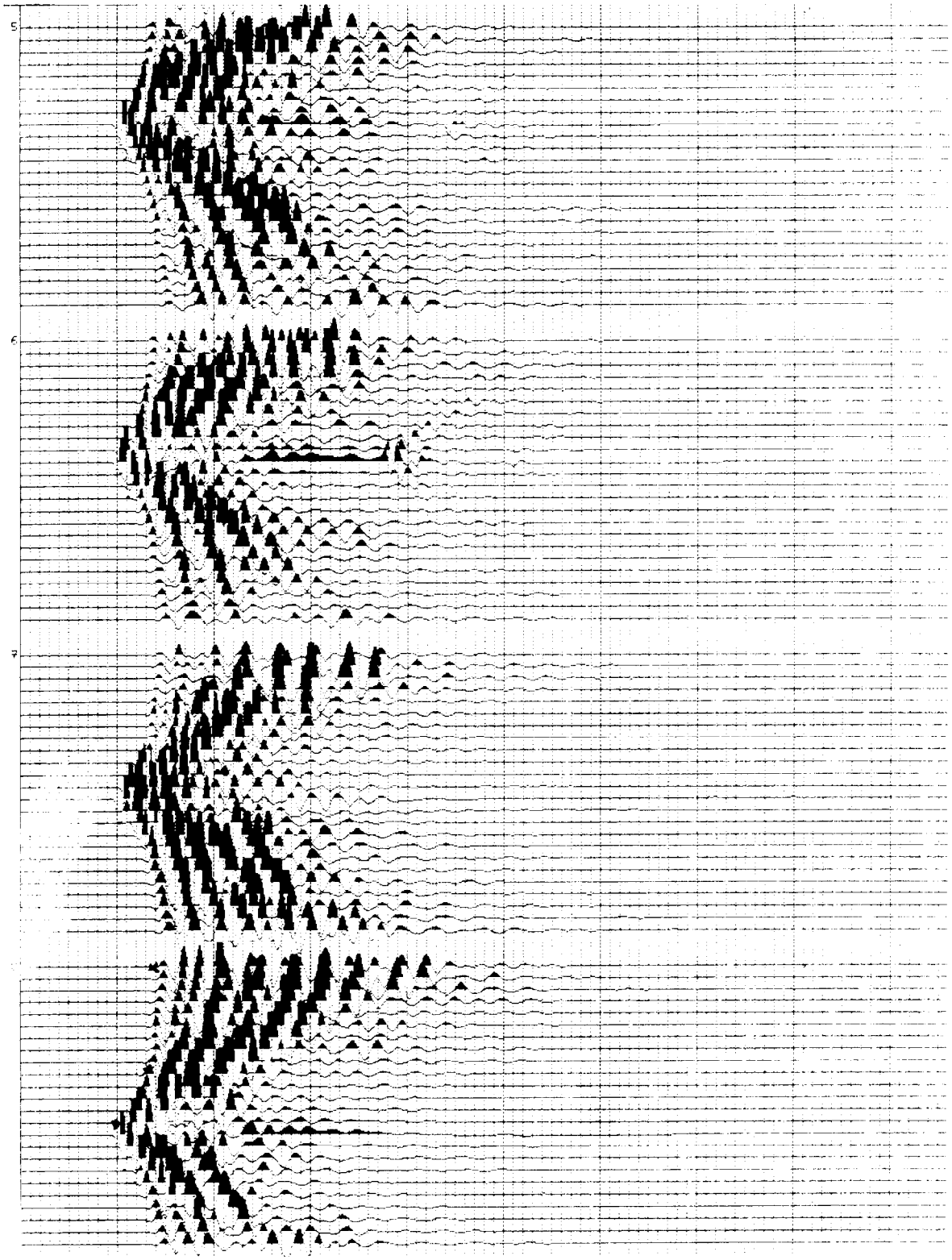

Figure B-1 continued. Tunnel 17, DRGW RR - Sum of 4 Dinoseis records.

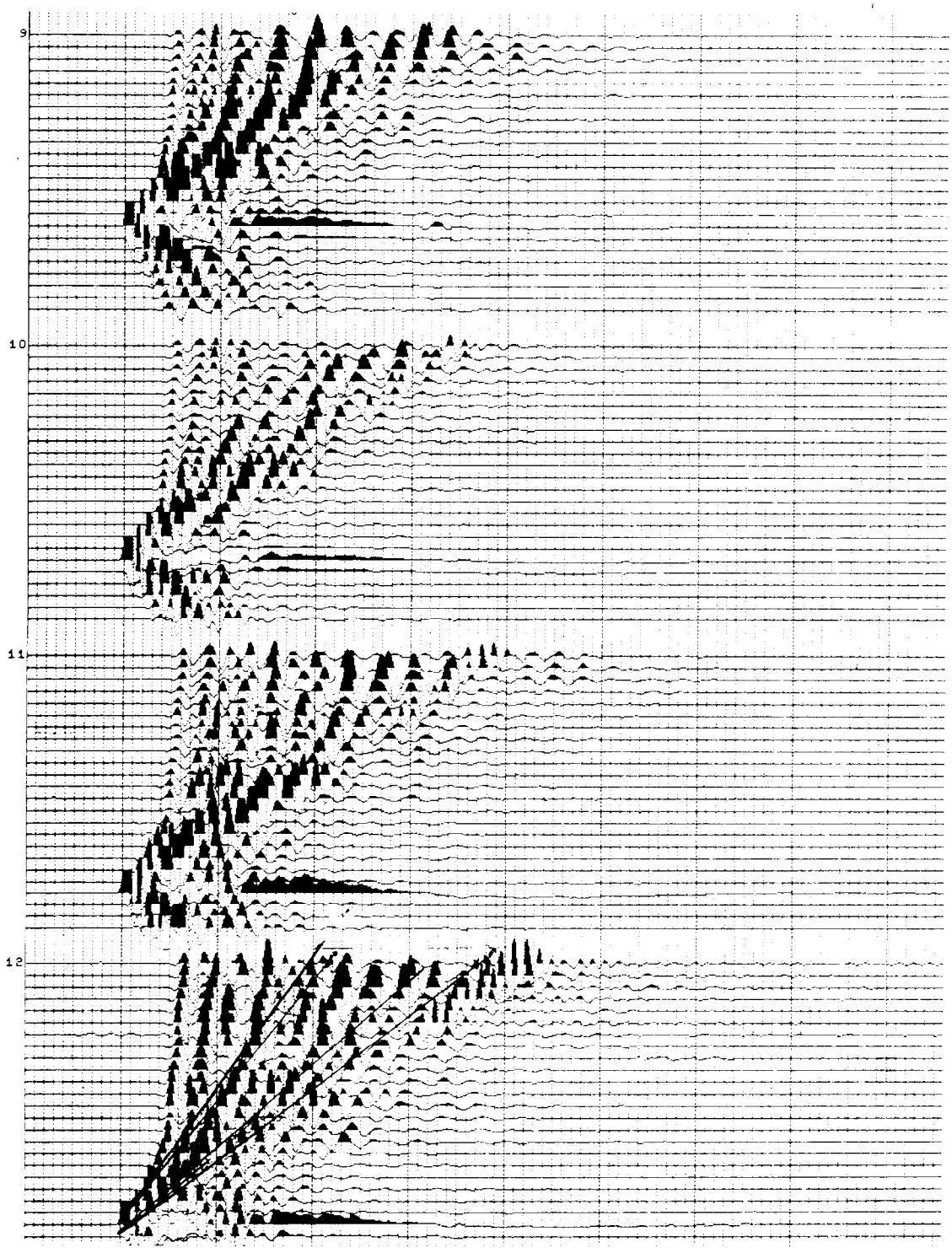

Figure B-1 continued. Tunnel 17, DRGW RR - Sum of 4 Dinoseis records.

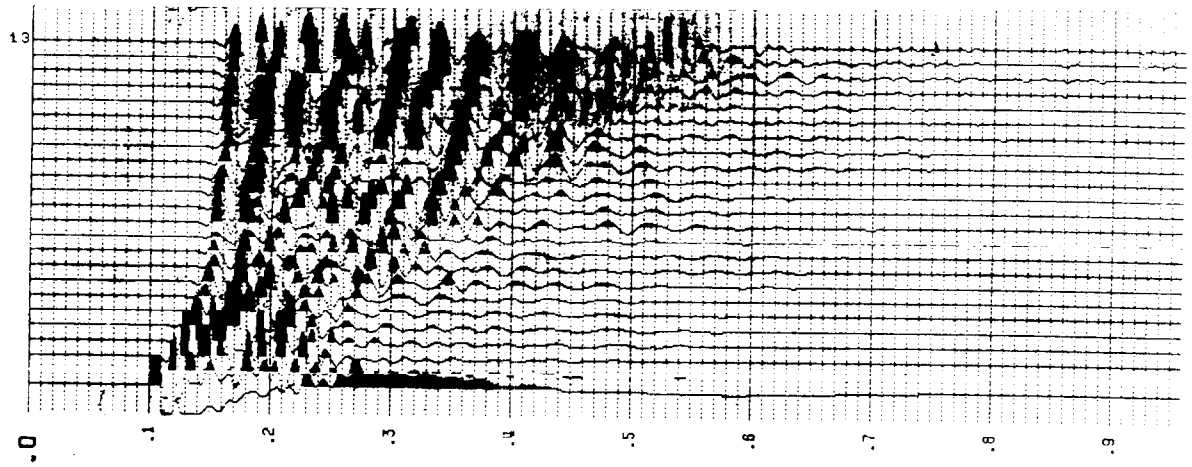

Figure B-1 continued. Tunnel 17, DRGW RR - Sum of 4 Dinoseis records.

```
HORIZONTAL PLOT RUNNING
SYS200A

**** PHOENIX LINE HEADER ***
  JOB ID NO.          14
  LINE NO.             1
  NO OF SAMPLES      500
  SAMPLING RATE        2
  CHANNELS/GROUP      24
  INPUT CREATED   SYS200A

  INPUT REEL NO     1099

XC
FORTRAN IV DN393944 REV.H
START GAIN (DB)   -33
```

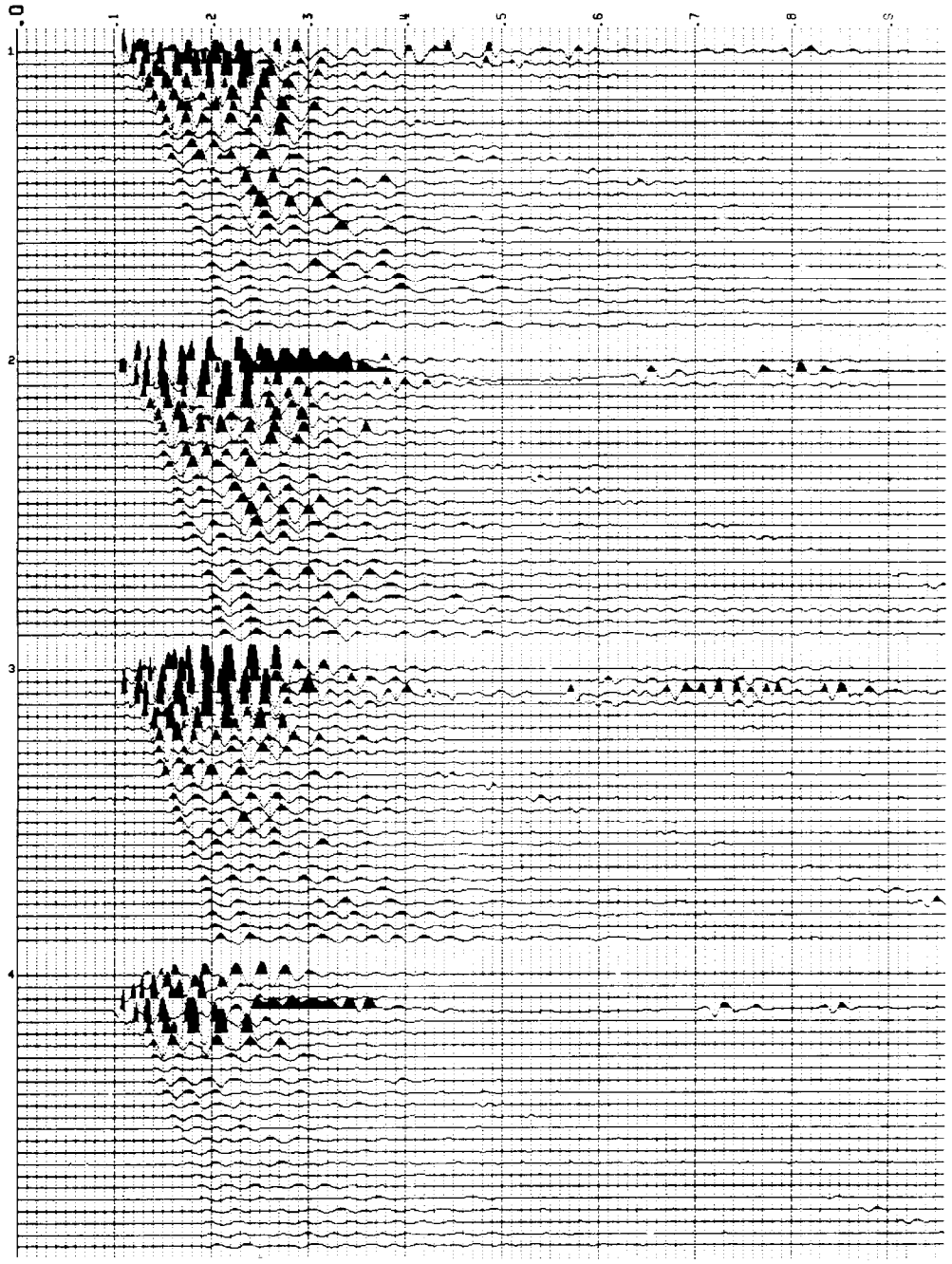

Figure B-2. Tunnel 19, DRGW RR - Sum of 4 Dinoseis records at each shot point. Static corrections added to align 1st breaks. Data time origin at 0.1 seconds.

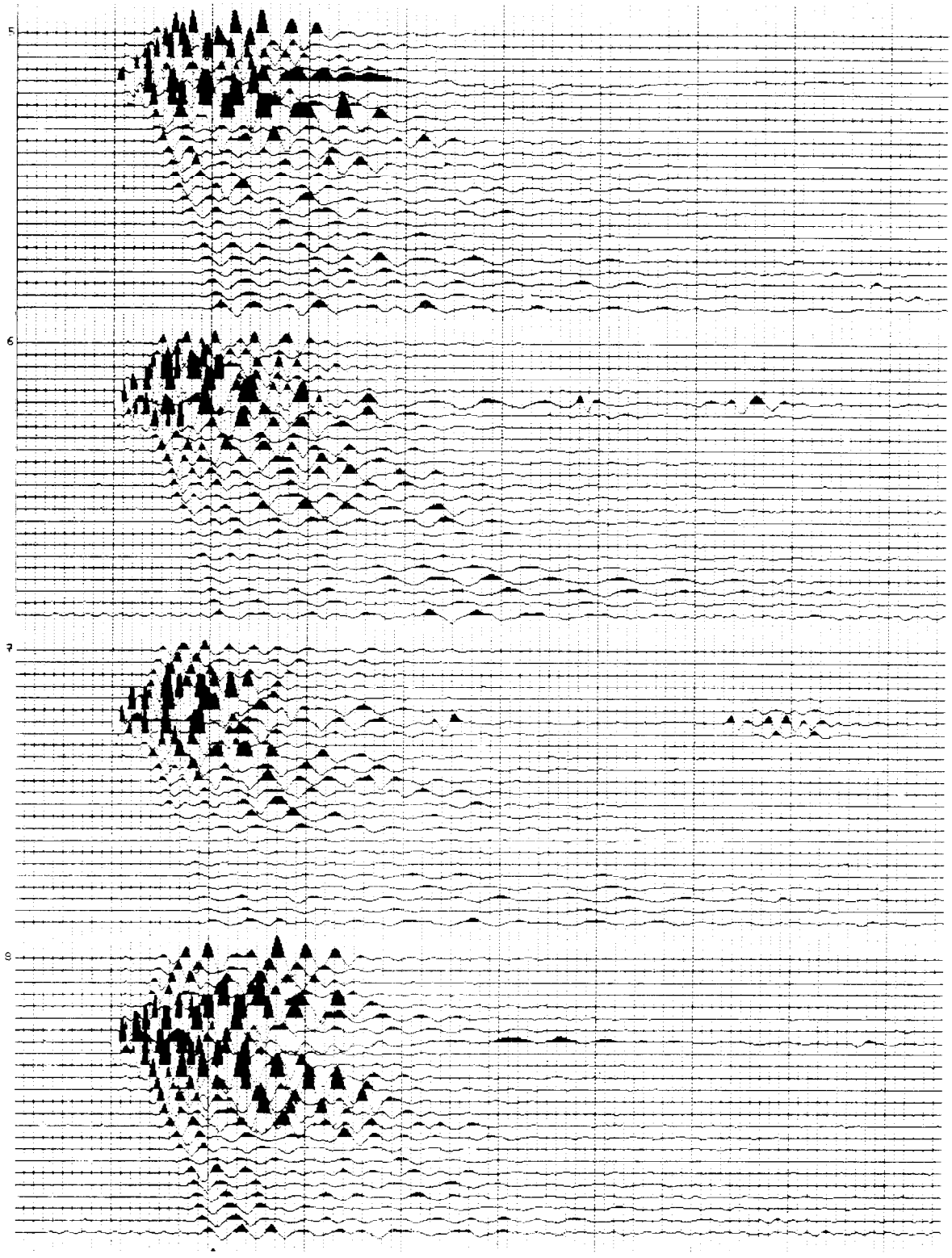

Figure B-2 continued. Tunnel 19, DRGW RR - Sum of 4 Dinoseis records.

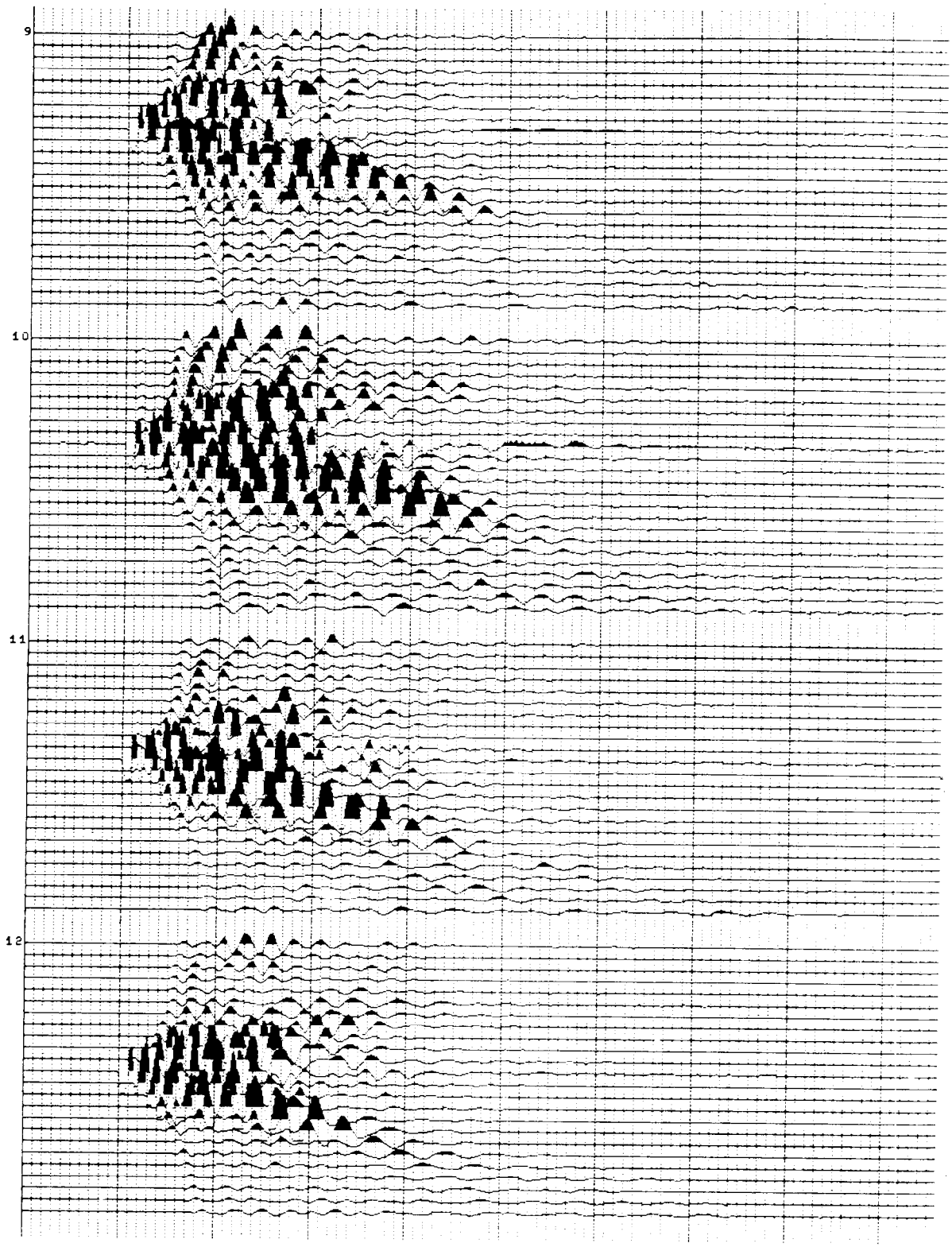

Figure B-2 continued. Tunnel 19, DRGW RR - Sum of 4 Dinoseis records.

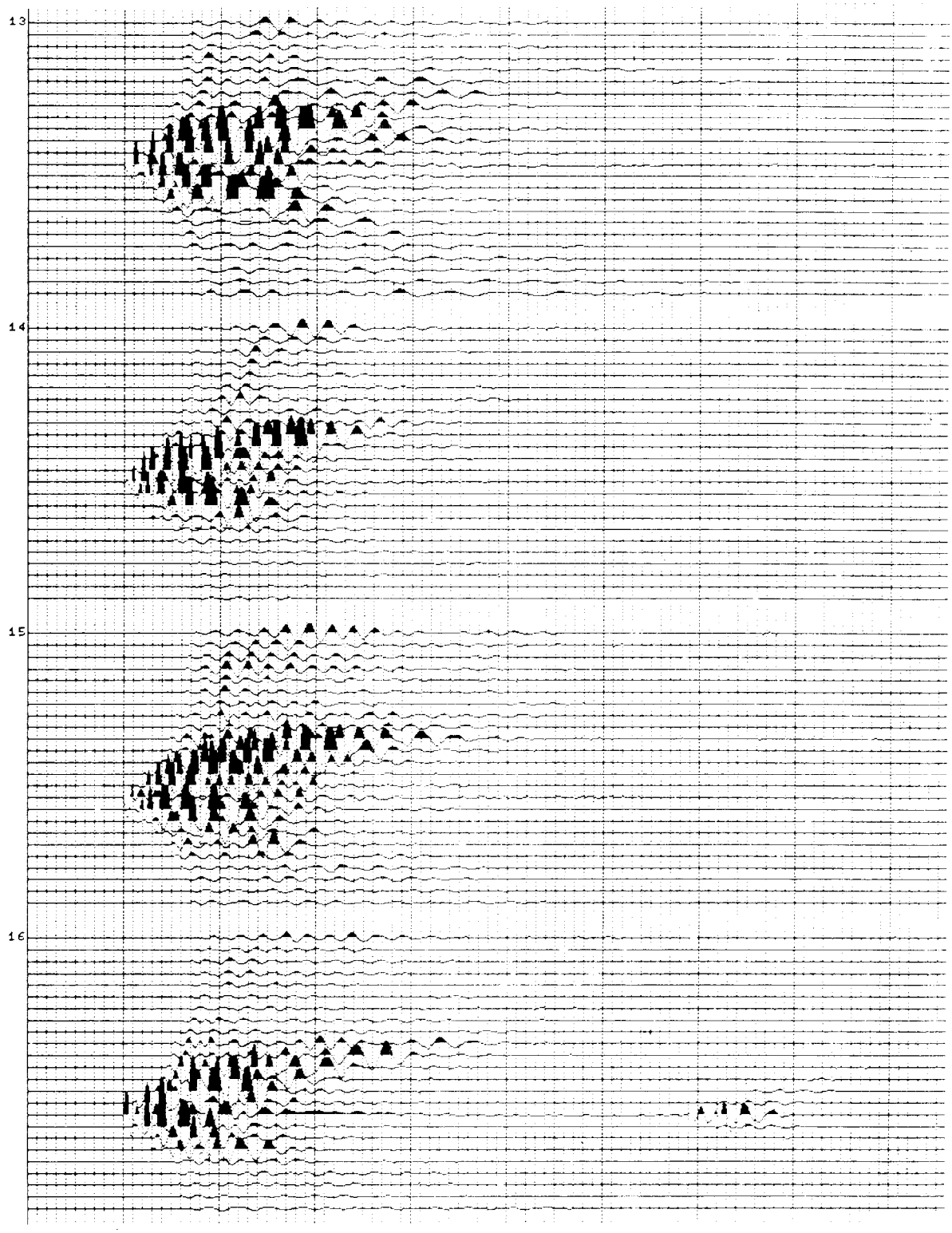

Figure B-2 continued. Tunnel 19, DRGW RR - Sum of 4 Dinoseis records.

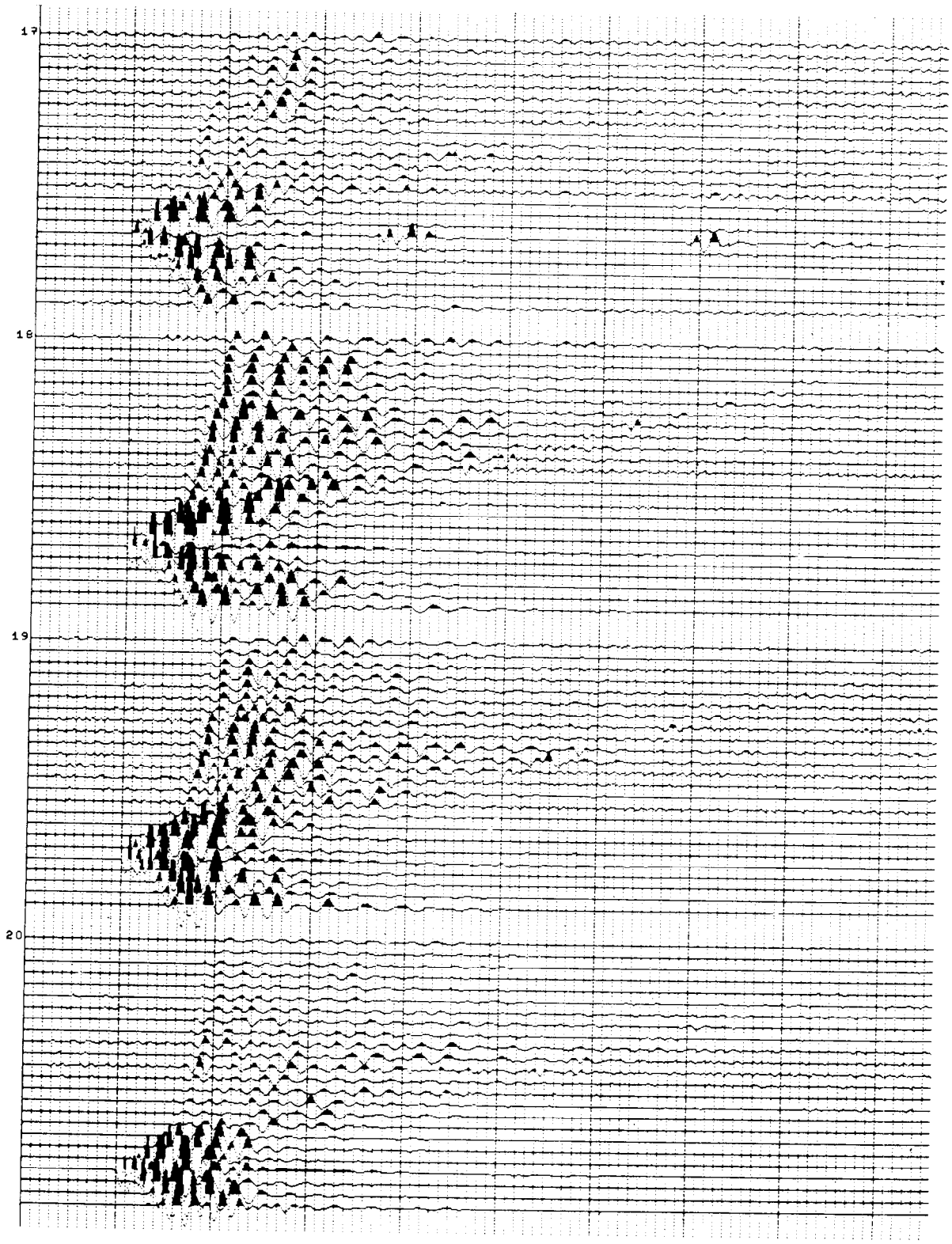

Figure B-2 continued. Tunnel 19, DRGW RR - Sum of 4 Dinoseis records.

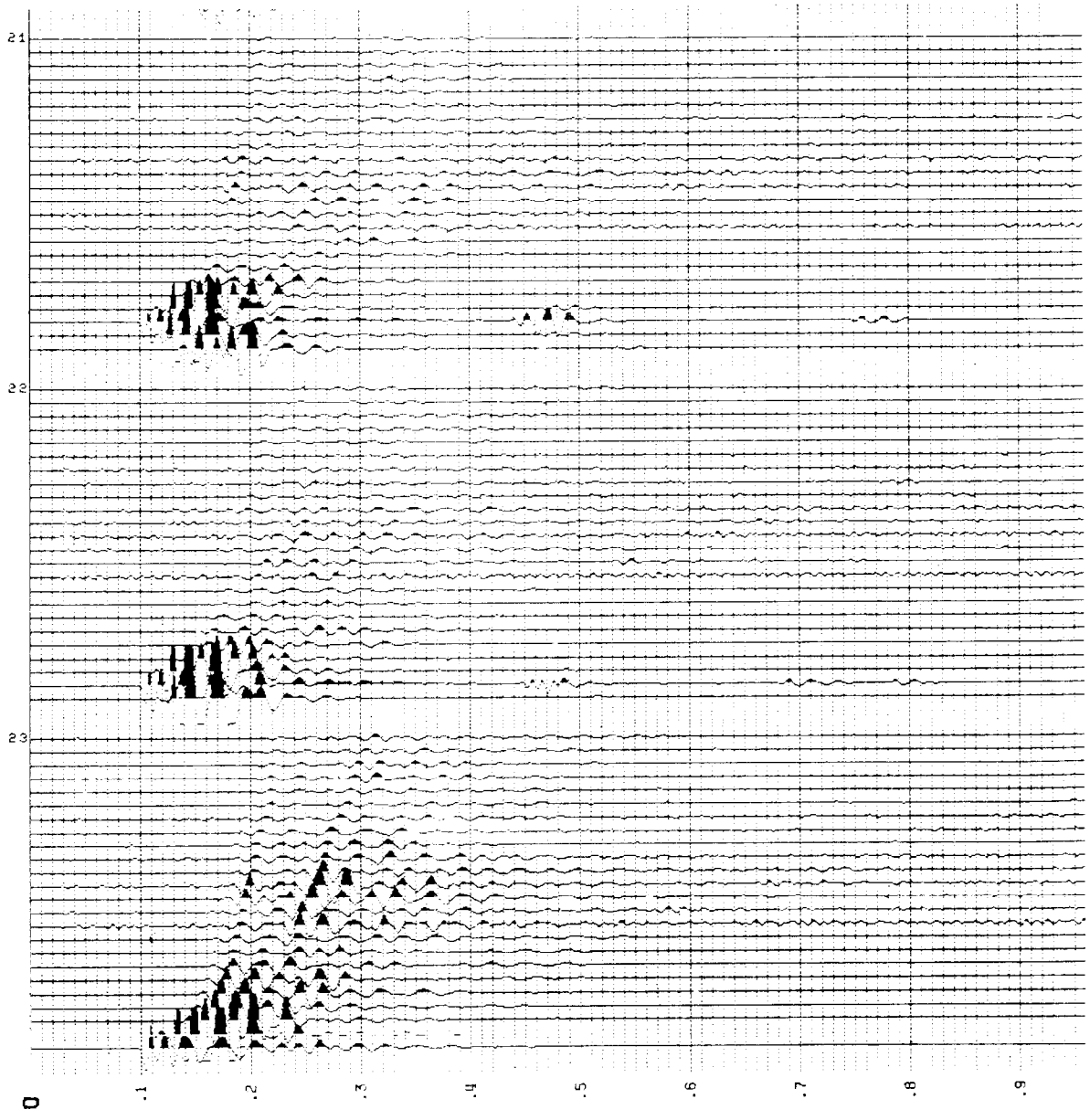

Figure B-2 continued. Tunnel 19, DRGW RR - Sum of 4 Dinoseis records.